

Computational Discovery and Optimization of a Potent, Selective, and Drug-like Scaffold for p38 α Inhibition

Jochem Nelen^{1,2}, Márcia Inês Goettert³, Michael Forster³, Laure Breuils⁴, José Manuel Villalgordo-Soto⁵, Stefan Laufer^{3,*} and Horacio Pérez-Sánchez^{1,*}

¹Structural Bioinformatics and High Performance Computing Research Group (BIO-HPC), UCAM HiTech, Universidad Católica de Murcia UCAM, Guadalupe, Murcia, 30107, Spain

²Health Sciences PhD Program, Universidad Católica de Murcia UCAM, Guadalupe, Murcia, 30107, Spain

³Department of Pharmaceutical/Medicinal Chemistry, Eberhard Karls University Tübingen, Tübingen, 72076, Germany

⁴Eurofins-Cerep S.A., Celle-Lévescault, 86600, France

⁵Eurofins-Villapharma Research, 30320 Murcia, Spain

* Email: stefan.laufer@uni-tuebingen.de

* Email: hperez@ucam.edu

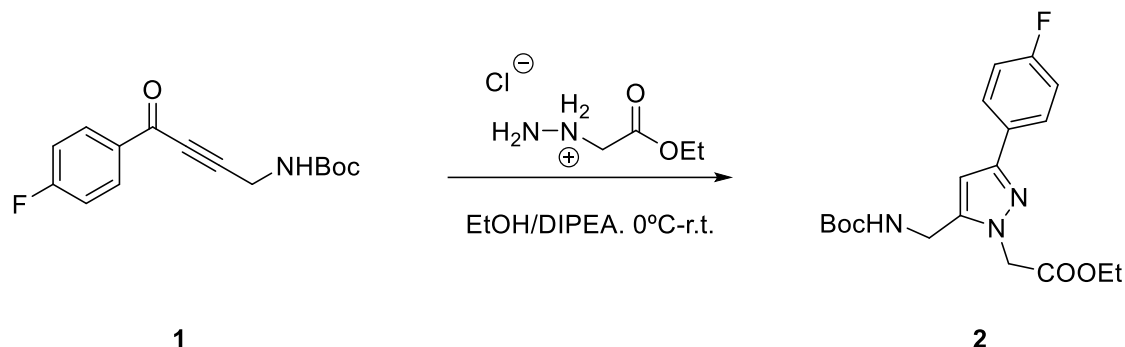
Table of Contents

Experimental Details.....	S3
Chemical Synthesis	S3
Representative Synthesis of Compound 26	S3
Supporting Analytical Data for Key Compounds	S7
Compound 26	S7
Compound 28	S9
Compound 47	S11
Compound 48	S13
Compound 50	S15
Compound 53	S17
ADMET Characterization	S19
Protein Binding.....	S19
Aqueous Solubility.....	S19
Partition Coefficient (LogD).....	S19
Caco-2 Permeability	S19
Half-life in Human Plasma	S19
Intrinsic Clearance.....	S20
CYP3A Inhibition	S20
Kinase Selectivity Assay	S20
Full MolSHAP Analysis of Substituent Contributions.....	S22
Full ADME Profiling Data of Key Compounds	S29
Full KINOMEScan Binding Profile of Compound 26	S36

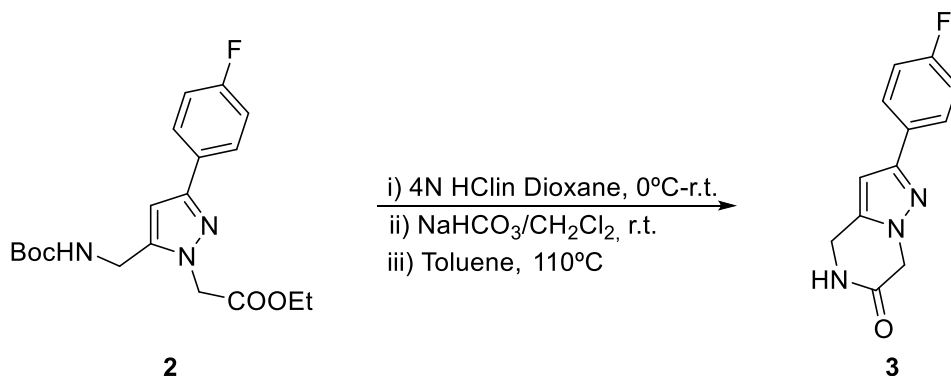
Experimental Details

Chemical Synthesis

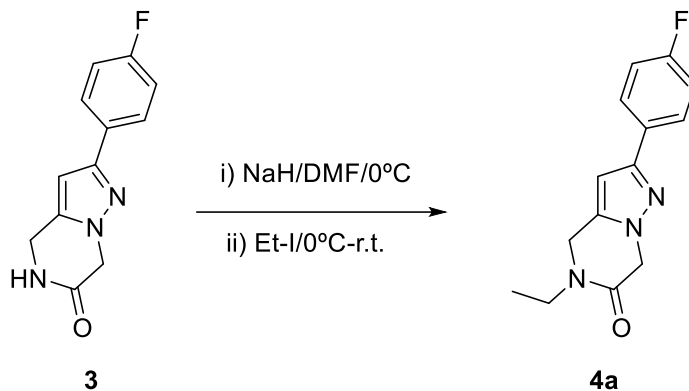
Representative Synthesis of Compound 26



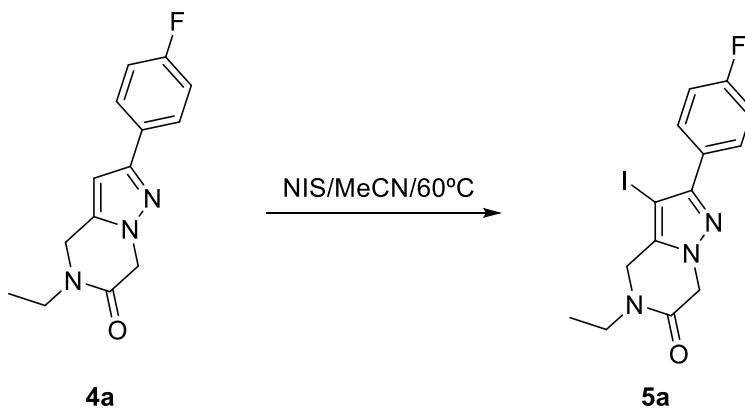
To a cooled (0°C) solution of the acetylenic ketone **1** (5 grs., 18.0 mmol) and the corresponding hydrazine hydrochloride (1.05 eq., 3.15 grs., 18.93 mmol) in EtOH (55 mL), DIPEA (1.05 eq., 18.93 mmol, 3.262 mL) was slowly added over a period of 1 hr. The reaction mixture was stirred at 0°C for 3 hr. The mixture is allowed to warm up to r.t. and further stirred for 2 hr. until total completion (TLC monitoring). The reaction mixture was concentrated under reduced pressure. The crude residue was partitioned between CH₂Cl₂ and Brine. The layers were separated, and the organic layer dried over MgSO₄, filtered and filtered through a plug of Celite/SiO₂. Evaporation under reduced pressure of CH₂Cl₂ afforded crude product **2** (6.336 grs., 93% yield) that was used in the next step without further purification.



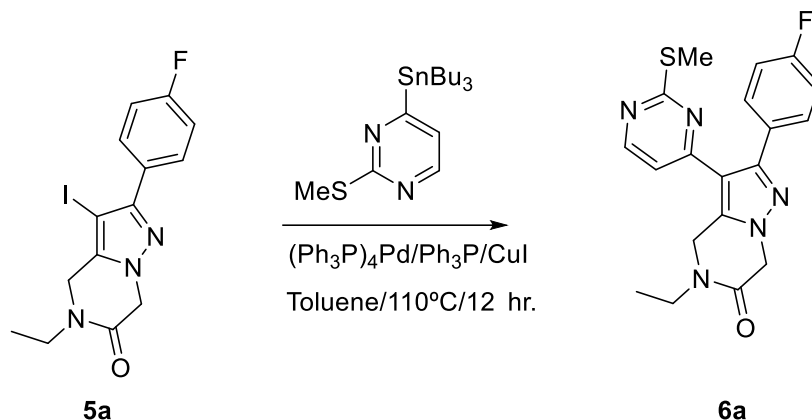
To pyrazole **2** (6.336 grs., 16.79 mmol), 50 mL of 4N HCl (in Dioxane) were added at r.t. The reaction mixture was stirred at r.t. overnight. Upon completion (TLC monitoring), the reaction mixture was concentrated under reduced pressure. The residue was partitioned between AcOEt and sat. solution of NaHCO₃. The layers were separated. The organic layer was washed with brine and separated. The organic layer was dried over MgSO₄, filtered and evaporated under reduced pressure. The resulting residue was diluted in toluene (50 mL) and refluxed for 2 hr. until cyclization was completed. Upon evaporation of the residue, the resulting residue was precipitated with toluene/MTBE to afford to a white solid **3** that was filtered and dried (2.64 gr., 68% yield)



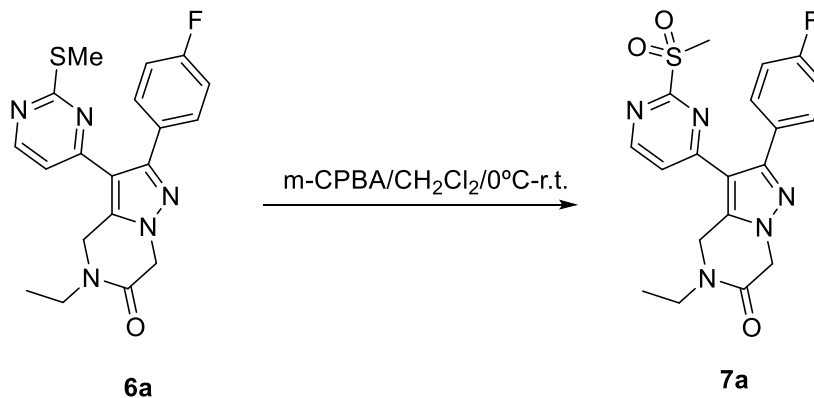
To a cooled (0°C) solution of **3** (3.1 gr., 13.41 mmol) in DMF (40 mL) NaH (1.50 eq., 20.12 mmol, 1.29 gr.) were added portionwise. The mixture was stirred at 0°C for 15 min. Ethyl iodide (1.20 eq., 16.09 mmol, 1.29 mL) were added dropwise. The reaction mixture was further stirred at r.t. overnight. Upon completion (TLC monitoring), H₂O (50 mL) was carefully added, and the mixture extracted with AcOEt (3x50 mL). The combined organic layers were dried over MgSO₄, filtered and concentrated under reduced pressure. The resulting residue was filtered through a short column of SiO₂ using CH₂Cl₂/MeOH mixtures to afford **4a** as a white solid (2.75 gr., 76% yield) that was used in the next step without further purification



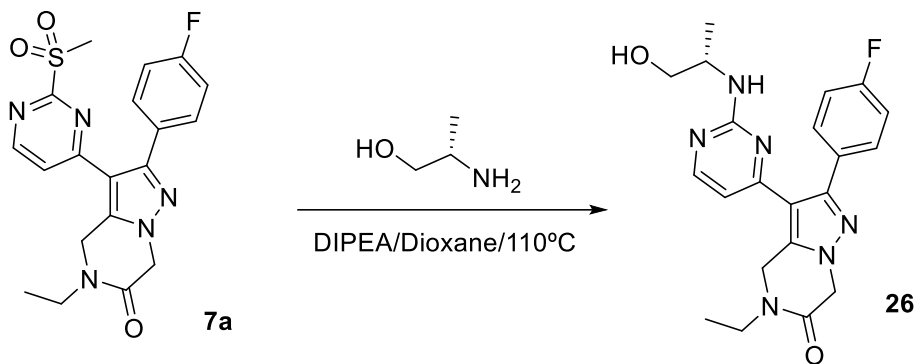
Compound **4a** (2.400 gr., 9.26 mmol) was dissolved in MeCN (100 mL), and protected from light. To this solution, NIS (2.20 eq., 20.37 mmol, 4.58 gr.) was added portionwise, and then allowed to react at 60°C for 16 hr. The solvent was evaporated and the residue filtered through a short column of SiO₂ (heptane/AcOEt mixtures) to afford **5a** (2.66 gr., 75% yield) as light yellow solid.



Compound **5a** (3.5 gr., 9.09 mmol), CuI (0.20 eq., 1.82 mmol, 347 mg), and PPh₃P (0.1 eq., 0.91 mmol, 240 mg) were dissolved in dry toluene (30 mL). A gentle stream of N₂ was passed through for 5 min. Then, tetrakis(triphenylphosphine)palladium (0.1 eq., 0.91 mmol, 1.052 gr.) was incorporated and the reaction mixture allowed to react at 110°C with good stirring overnight. Upon completion, H₂O (50 mL) were added and the mixture extracted with CH₂Cl₂ (3x40 mL). The combined organic layers were dried over MgSO₄, filtered and concentrated under reduced pressure. The resulting residue was filtered through a short column of SiO₂ (heptane/AcOEt mixtures) to afford **6a** (1.92 gr., 55% yield) as light brown solid.



To a cooled (0°C) solution of **6a** (1.8 gr., 4.69 mmol) in CH₂Cl₂ 50 mL), m-CPBA (2.80 eq., 13.13 mmol, 2.27 gr.), was added portion wise. The mixture was stirred from 0°C until r.t. overnight. Sat. Soln. of NaHCO₃ (50 mL) were added and the mixture extracted with CH₂Cl₂ (3x30 mL). The combined organic layers were dried over MgSO₄, filtered and concentrated under reduced pressure. The resulting residue was filtered through a short column of SiO₂ (CH₂Cl₂/MeOH mixtures) to afford **7a** (1.450 gr., 74% yield) as a yellow foam, that was used directly in the next step.



Sulfonyl derivative **7a** (750 mg, 1.81 mmol), amino alcohol (4 eq., 7.24 mmol, 0.57 mL) and DIPEA (4 eq., 7.24 mmol, 1.293 mL) were taken up in dioxane (10 mL). The mixture was stirred at 110°C overnight. Due to uncompletion, 2 additional eq. of amino alcohol and DIPEA were added and the mixture was stirred for additional 16 hr. Sat. solution of NH_4Cl was added and the mixture was extracted with EtOAc (3x15 mL). The combined organic layers were dried over MgSO_4 , filtered and evaporated under reduced pressure. The resulting was purified through MPLC on SiO_2 ($\text{CH}_2\text{Cl}_2/\text{MeOH}$) affording targeted compound **26** (420 mg, 57% Yield) as white solid.

Supporting Analytical Data for Key Compounds

Compound 26

(S)-5-ethyl-2-(4-fluorophenyl)-3-(2-((1-hydroxypropan-2-yl)amino)pyrimidin-4-yl)-4,5-dihydropyrazolo[1,5-a]pyrazin-6(7H)-one

^1H NMR (400 MHz, $\text{DMSO-}d_6$) δ ppm 8.02 - 8.07 (m, 1 H), 7.46 - 7.52 (m, 2 H), 7.23 - 7.31 (m, 2 H), 6.76 - 6.81 (m, 1 H), 6.11 (d, $J=5.15$ Hz, 1 H), 4.91 - 4.97 (m, 2 H), 4.81 - 4.86 (m, 2 H), 4.68 - 4.72 (m, 1 H), 3.91 - 4.02 (m, 1 H), 3.47 - 3.55 (m, 2 H), 3.32 - 3.37 (m, 1 H), 1.13 - 1.19 (m, 6 H). $[\text{M}+\text{H}]^+ = 411.15$, calculated exact mass for $\text{C}_{21}\text{H}_{24}\text{FN}_6\text{O}_2 = 411.19$; purity 96%; $t_{\text{R}} = 2.162$ min.

^1H NMR (400 MHz, $\text{DMSO-}d_6$) δ ppm 8.02 - 8.07 (m, 1 H), 7.46 - 7.52 (m, 2 H), 7.23 - 7.31 (m, 2 H), 6.76 - 6.81 (m, 1 H), 6.11 (d, $J=5.15$ Hz, 1 H), 4.91 - 4.97 (m, 2 H), 4.81 - 4.86 (m, 2 H), 4.68 - 4.72 (m, 1 H), 3.91 - 4.02 (m, 1 H), 3.47 - 3.55 (m, 2 H), 3.32 - 3.37 (m, 1 H), 1.13 - 1.19 (m, 6 H)

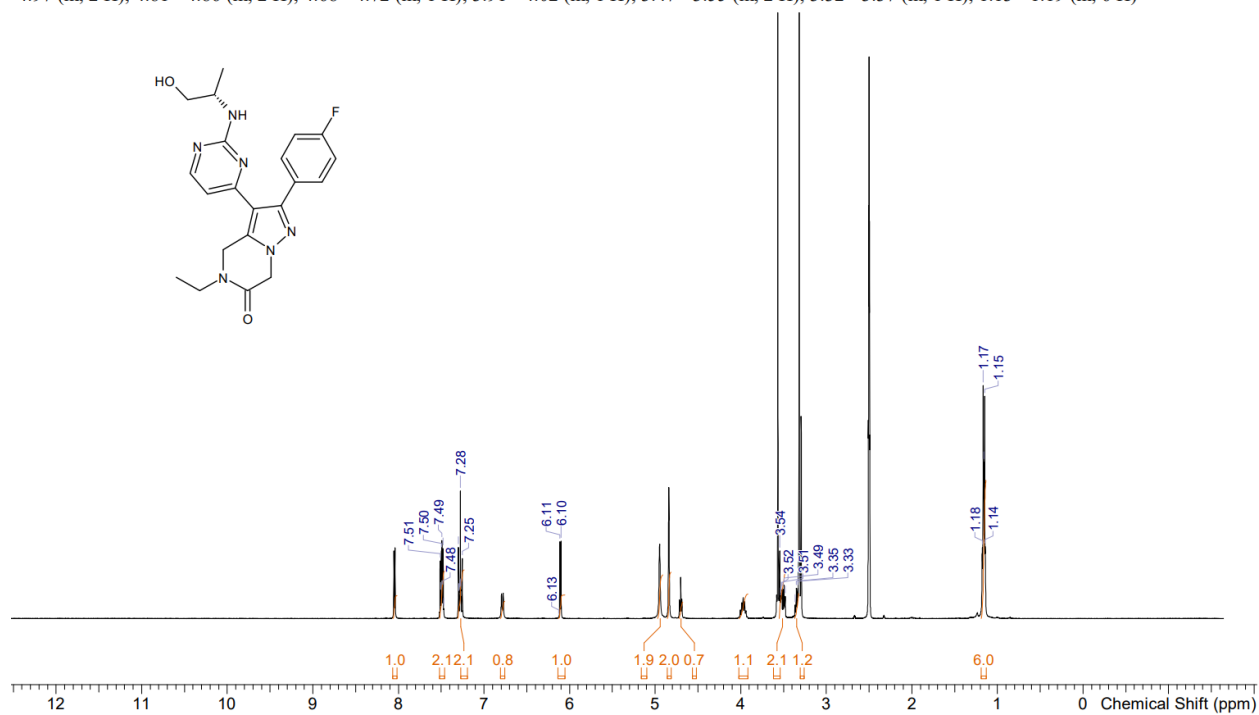
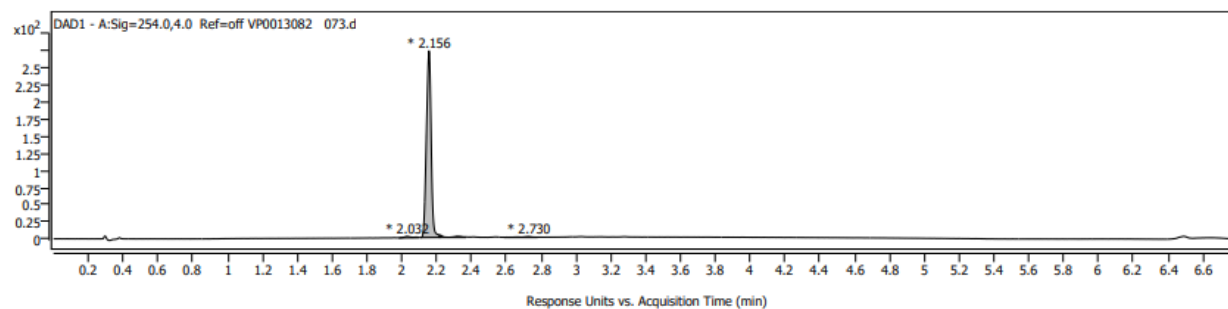
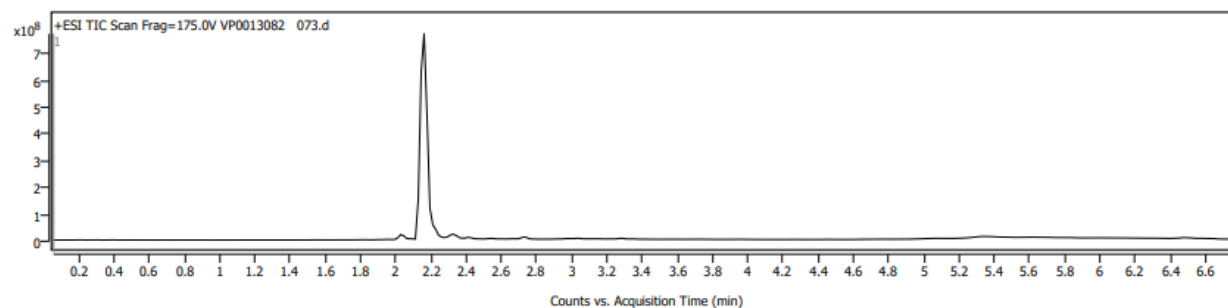


Figure S1.A ^1H NMR (400 MHz, $\text{DMSO-}d_6$) spectra of Compound 26.

Sample Chromatograms

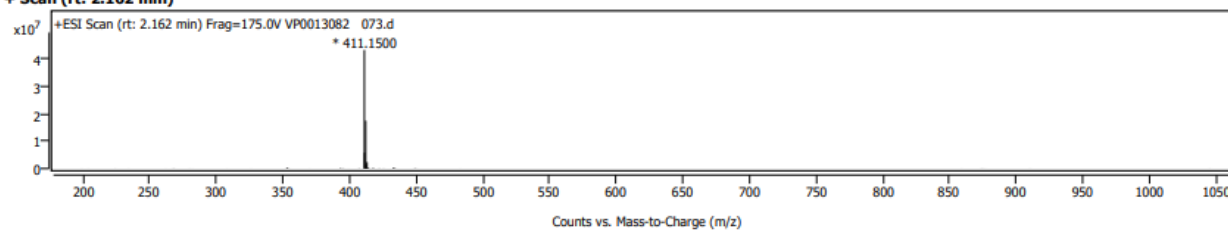


Chromatogram Peaks

Peak	Start	RT	End	Height	Area	Area Sum %
1	1.986	2.032	2.092	2	6	1.15
2	2.108	2.156	2.216	273	515	96.03
3	2.218	2.220	2.364	3	9	1.71
4	2.591	2.730	2.775	1	6	1.11

Sample Spectra

+ Scan (rt: 2.162 min)



Spectrum Peaks

m/z	Z	Abund	Abund %	m/z (Calc)	Diff (ppm)	Ion Species	Formula	Ion Type
411.1500	1	43319904	100.00					
411.3192	1	5771208	13.32					
412.1470	1	17504536	40.41					
412.3218	1	1414774	3.27					
413.1486	1	2361351	5.45					

Figure S1.B LC-MS spectra for Compound 26.

Compound 28

(S)-2-(4-fluorophenyl)-3-(2-((1-hydroxypropan-2-yl)amino)pyrimidin-4-yl)-5-propyl-4,5-dihydropyrazolo[1,5-a]pyrazin-6(7H)-one

^1H NMR (400 MHz, $\text{DMSO-}d_6$) δ ppm 8.01 - 8.06 (m, 1 H), 7.45 - 7.52 (m, 2 H), 7.24 - 7.31 (m, 2 H), 6.78 (br d, $J=8.01$ Hz, 1 H), 6.11 (d, $J=5.15$ Hz, 1 H), 4.95 (br s, 2 H), 4.85 (s, 2 H), 3.92 - 4.00 (m, 1 H), 3.45 - 3.52 (m, 3 H), 1.62 (sxt, $J=7.38$ Hz, 2 H), 1.15 (d, $J=6.68$ Hz, 3 H), 0.89 (t, $J=7.39$ Hz, 3 H). $[\text{M}+\text{H}]^+ = 425.16$, calculated exact mass for $\text{C}_{22}\text{H}_{26}\text{FN}_6\text{O}_2 = 425.21$; purity 95%; $t_{\text{R}} = 2.325$ min.

^1H NMR (400 MHz, $\text{DMSO-}d_6$) δ ppm 8.01 - 8.06 (m, 1 H), 7.45 - 7.52 (m, 2 H), 7.24 - 7.31 (m, 2 H), 6.78 (br d, $J=8.01$ Hz, 1 H), 6.11 (d, $J=5.15$ Hz, 1 H), 4.95 (br s, 2 H), 4.85 (s, 2 H), 3.92 - 4.00 (m, 1 H), 3.45 - 3.52 (m, 3 H), 1.62 (sxt, $J=7.38$ Hz, 2 H), 1.15 (d, $J=6.68$ Hz, 3 H), 0.89 (t, $J=7.39$ Hz, 3 H)

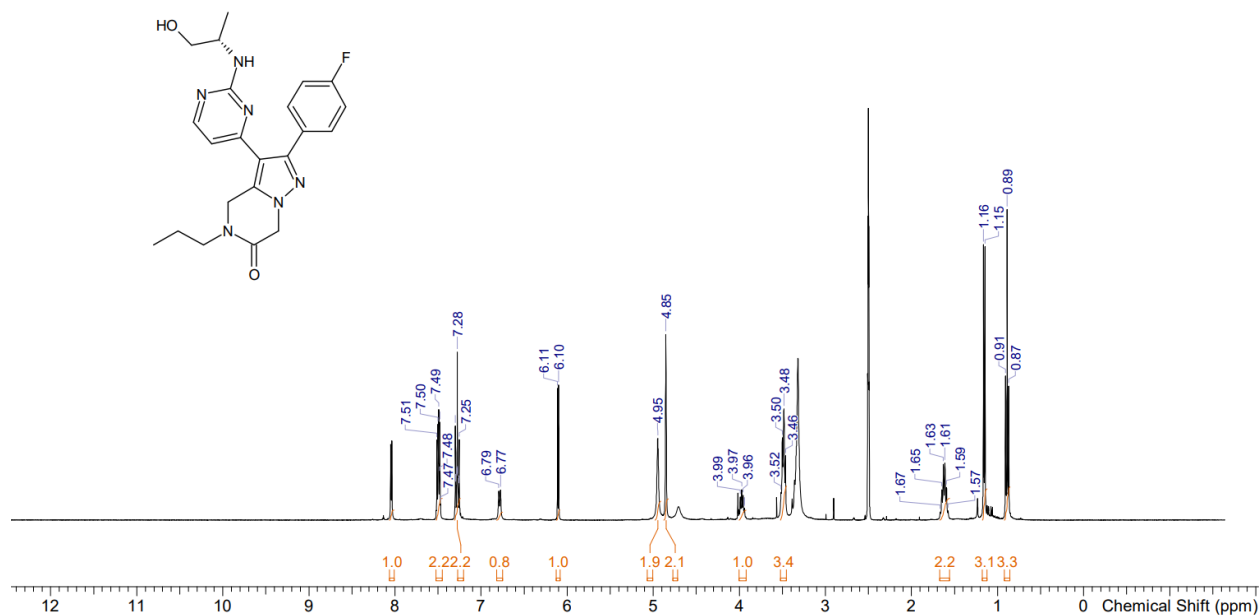
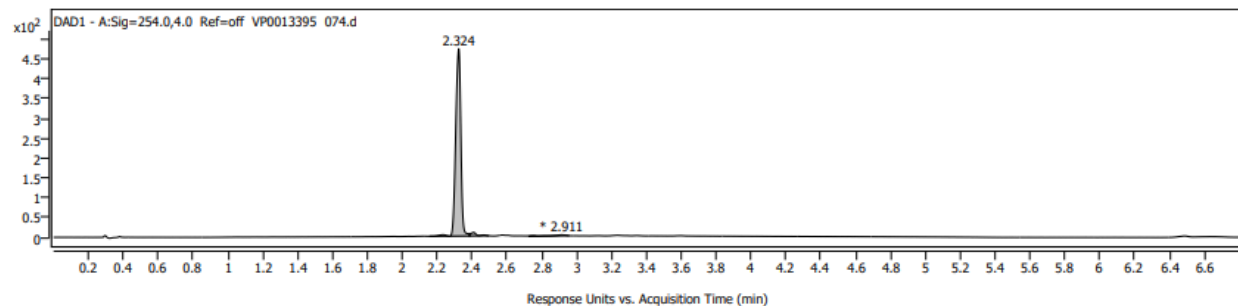
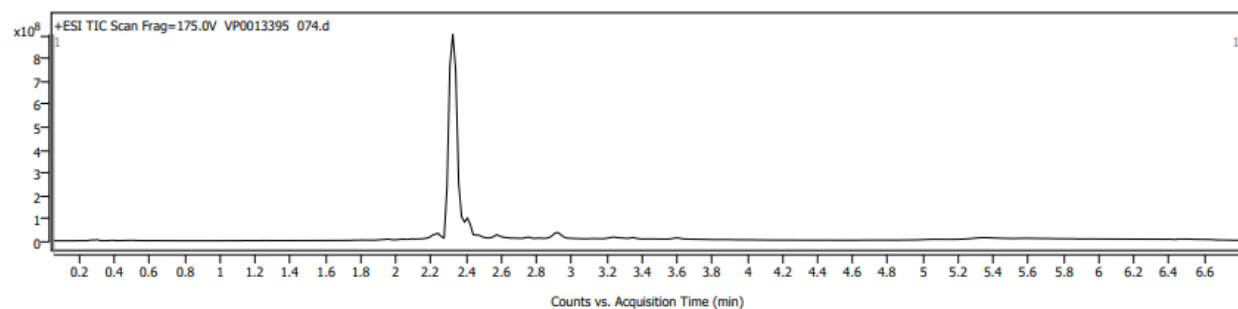


Figure S2.A ^1H NMR (400 MHz, $\text{DMSO-}d_6$) spectra of Compound 28.

Sample Chromatograms

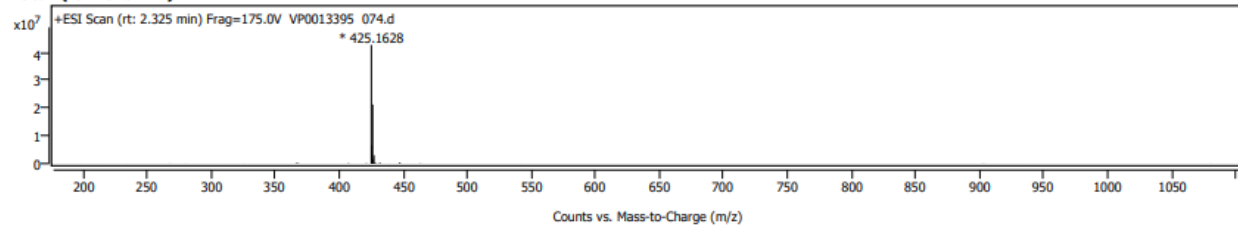


Chromatogram Peaks

Peak	Start	RT	End	Height	Area	Area Sum %
1	2.157	2.233	2.270	4	11	1.10
2	2.273	2.324	2.386	473	959	94.78
3	2.386	2.409	2.497	9	22	2.17
4	2.727	2.911	2.957	3	20	1.95

Sample Spectra

+ Scan (rt: 2.325 min)



Spectrum Peaks

m/z	Z	Abund	Abund %	m/z (Calc)	Diff (ppm)	Ion Species	Formula	Ion Type
425.1628	1	42616120	100.00					
425.3327	1	6530169	15.32					
426.1576	1	21190336	49.72					
426.3334	1	1681772	3.95					
427.1588	1	2983364	7.00					

Figure S2.B LC-MS spectra for Compound 28.

Compound 47

(S)-2-(4-fluorophenyl)-3-(2-((1-phenylethyl)amino)pyrimidin-4-yl)-4,5-dihydropyrazolo[1,5-a]pyrazin-6(7H)-one

^1H NMR (400 MHz, $\text{DMSO}-d_6$) δ ppm 8.58 (br s, 1 H), 7.99 - 8.07 (m, 1 H), 7.65 (br d, $J=8.01$ Hz, 1 H), 7.42 - 7.48 (m, 2 H), 7.36 - 7.41 (m, 2 H), 7.30 (t, $J=7.63$ Hz, 2 H), 7.25 (t, $J=8.92$ Hz, 2 H), 7.20 (d, $J=7.34$ Hz, 1 H), 6.09 (d, $J=5.15$ Hz, 1 H), 4.96 - 5.09 (m, 1 H), 4.72 - 4.81 (m, 3 H), 1.43 (d, $J=6.96$ Hz, 3 H). $[\text{M}+\text{H}]^+ = 429.13$, calculated exact mass for $\text{C}_{24}\text{H}_{22}\text{FN}_6\text{O} = 429.18$; purity 99%; $t_{\text{R}} = 2.895$ min.

^1H NMR (400 MHz, $\text{DMSO}-d_6$) δ ppm 8.58 (br s, 1 H), 7.99 - 8.07 (m, 1 H), 7.65 (br d, $J=8.01$ Hz, 1 H), 7.42 - 7.48 (m, 2 H), 7.36 - 7.41 (m, 2 H), 7.30 (t, $J=7.63$ Hz, 2 H), 7.25 (t, $J=8.92$ Hz, 2 H), 7.20 (d, $J=7.34$ Hz, 1 H), 6.09 (d, $J=5.15$ Hz, 1 H), 4.96 - 5.09 (m, 1 H), 4.72 - 4.81 (m, 3 H), 1.43 (d, $J=6.96$ Hz, 3 H)

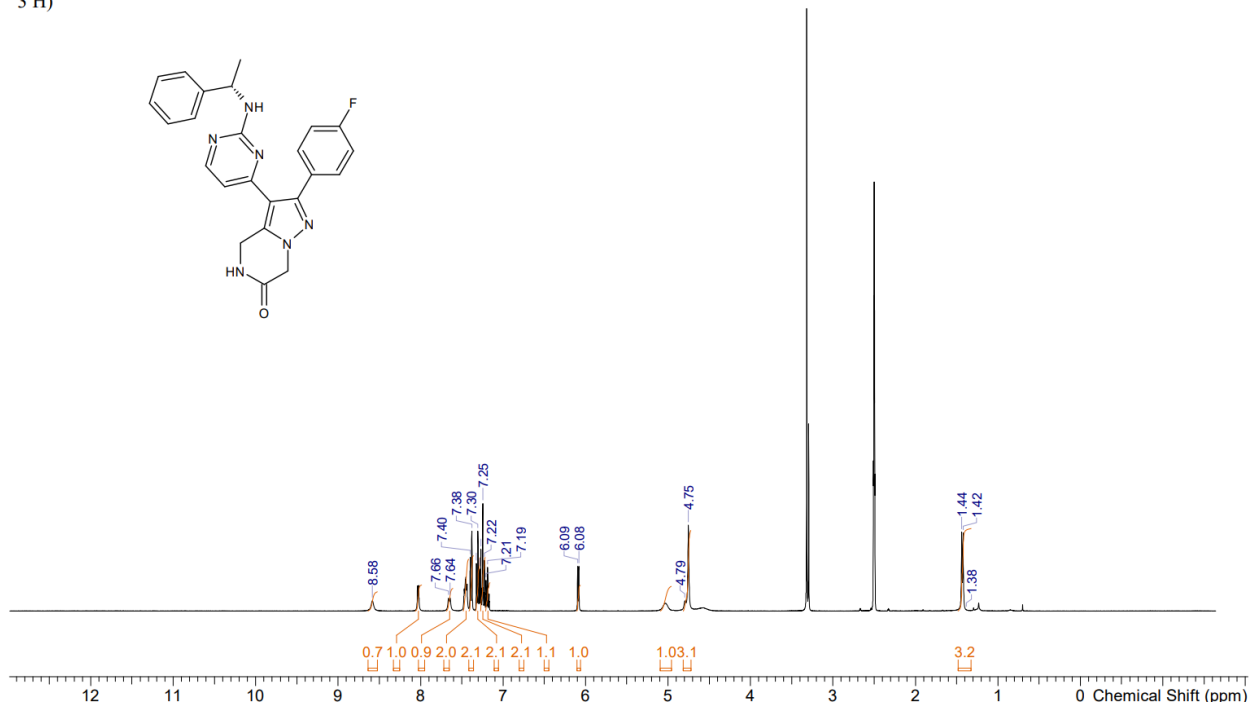
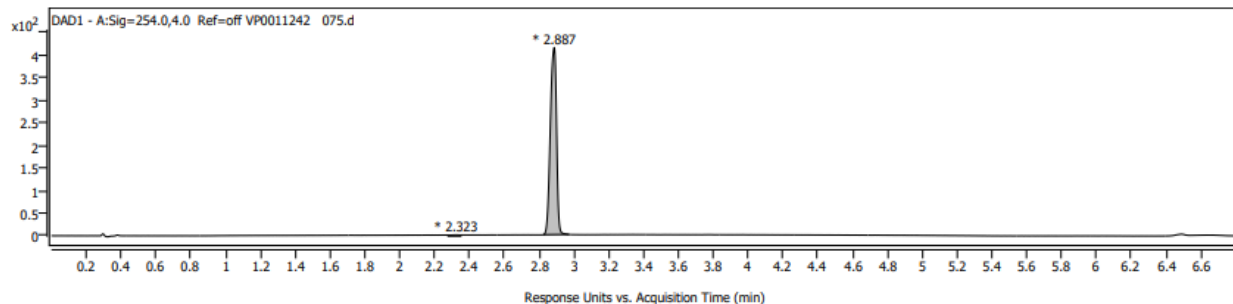
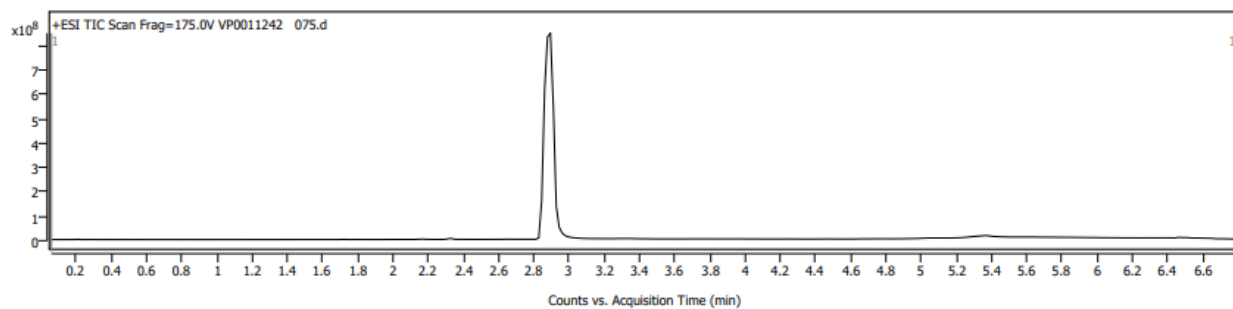


Figure S3.A ^1H NMR (400 MHz, $\text{DMSO}-d_6$) spectra of Compound 47.

Sample Chromatograms

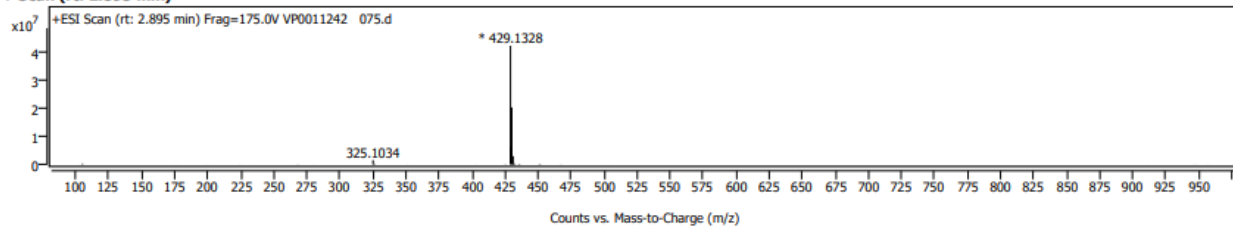


Chromatogram Peaks

Peak	Start	RT	End	Height	Area	Area Sum %
1	2.278	2.323	2.350	3	10	0.99
2	2.824	2.887	2.972	415	1025	99.01

Sample Spectra

+ Scan (rt: 2.895 min)



Spectrum Peaks

m/z	Z	Abund	Abund %	m/z (Calc)	Diff (ppm)	Ion Species	Formula	Ion Type
325.1034		1461586	3.48					
429.1328	1	41980840	100.00					
429.3026	1	6107177	14.55					
430.1291	1	20124236	47.94					
430.3093	1	1593661	3.80					
431.1307	1	2883134	6.87					

Figure S3.B LC-MS spectra for Compound 47.

Compound 48

2-(4-fluorophenyl)-3-(2-(isopropylamino)pyrimidin-4-yl)-4,5-dihydropyrazolo[1,5-a]pyrazin-6(7H)-one

^1H NMR (400 MHz, $\text{DMSO}-d_6$) δ ppm 7.97 - 8.07 (m, 1 H), 7.42 - 7.51 (m, 2 H), 7.22 - 7.30 (m, 2 H), 6.08 (d, $J=5.15$ Hz, 1 H), 4.77 (br d, $J=2.57$ Hz, 4 H), 3.92 - 4.02 (m, 1 H), 1.14 (d, $J=6.48$ Hz, 6 H). $[\text{M}+\text{H}]^+ = 367.14$, calculated exact mass for $\text{C}_{19}\text{H}_{20}\text{FN}_6\text{O} = 367.17$; purity 96%; $t_R = 2.164$ min.

^1H NMR (400 MHz, $\text{DMSO}-d_6$) δ ppm 7.97 - 8.07 (m, 1 H), 7.42 - 7.51 (m, 2 H), 7.22 - 7.30 (m, 2 H), 6.08 (d, $J=5.15$ Hz, 1 H), 4.77 (br d, $J=2.57$ Hz, 4 H), 3.92 - 4.02 (m, 1 H), 1.14 (d, $J=6.48$ Hz, 6 H)

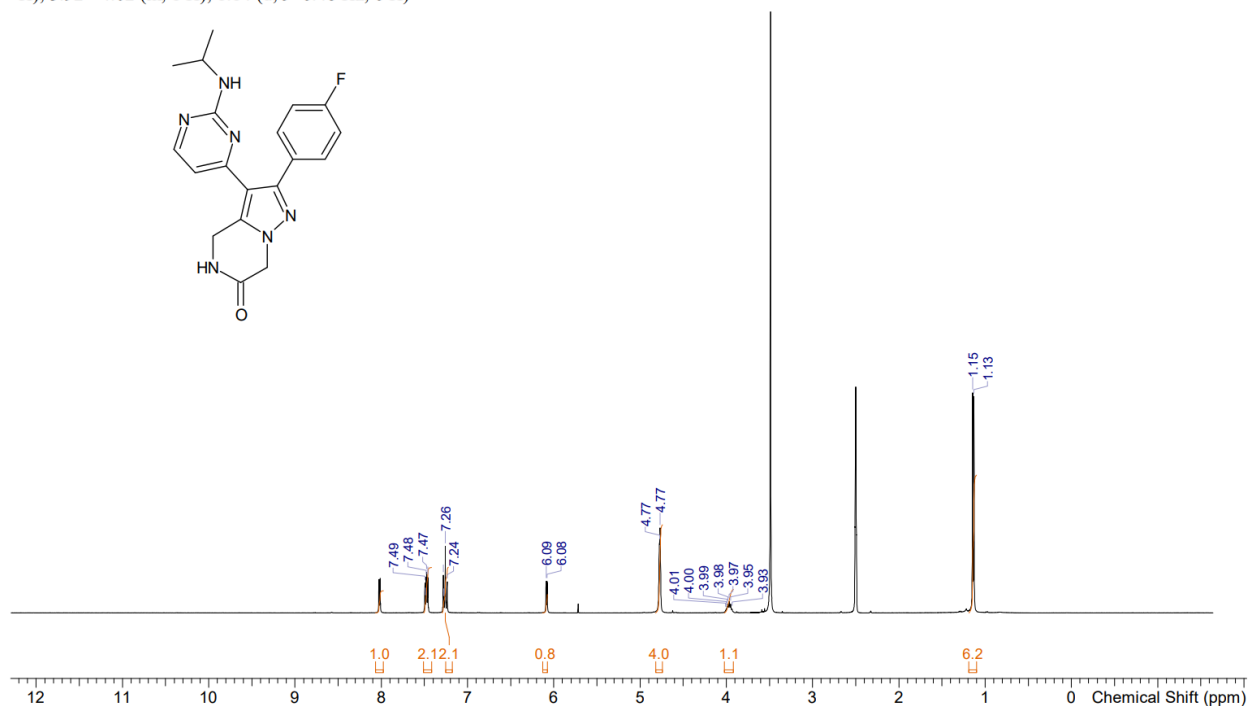
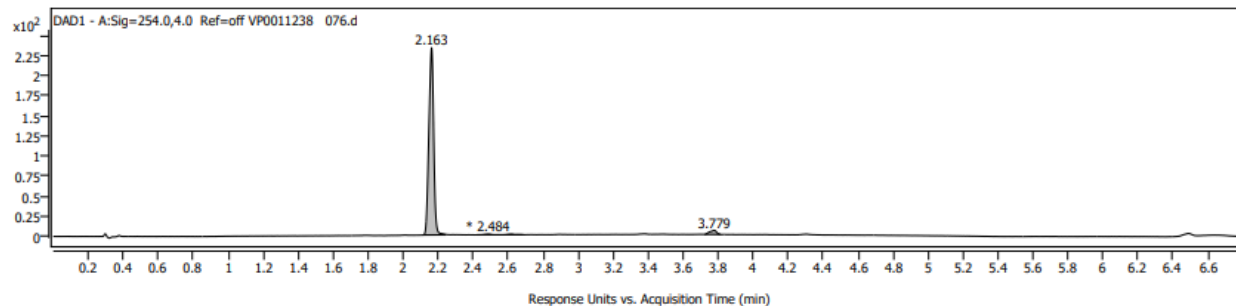
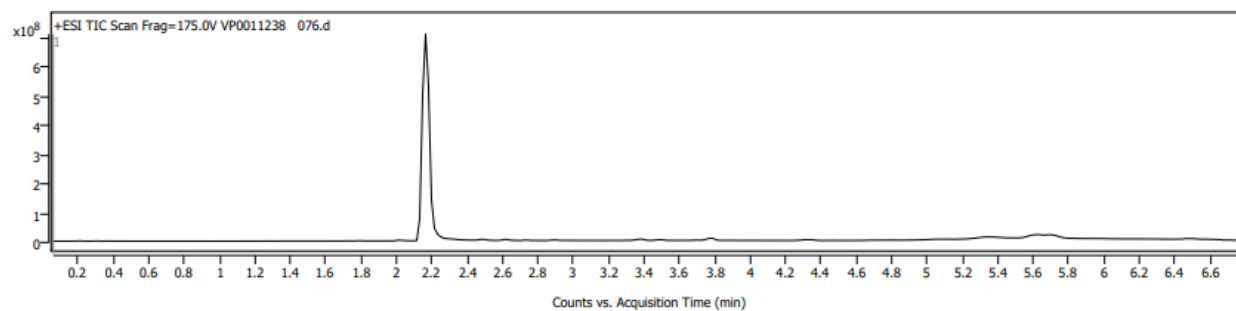


Figure S4.A ^1H NMR (400 MHz, $\text{DMSO}-d_6$) spectra of Compound 48.

Sample Chromatograms

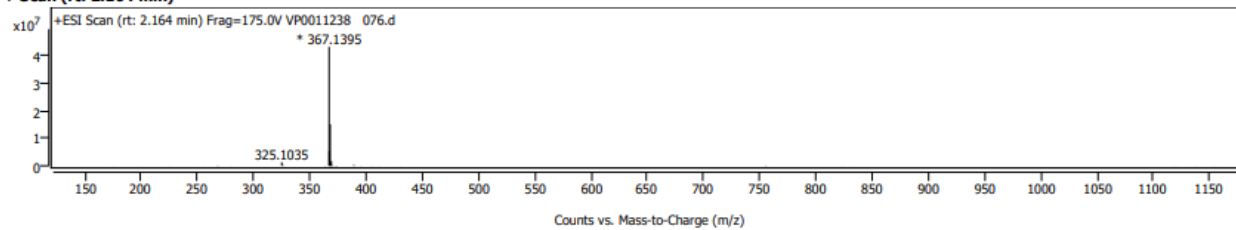


Chromatogram Peaks

Peak	Start	RT	End	Height	Area	Area Sum %
1	2.116	2.163	2.241	233	443	95.92
2	2.423	2.484	2.687	1	5	1.10
3	3.725	3.779	3.814	5	14	2.97

Sample Spectra

+ Scan (rt: 2.164 min)



Spectrum Peaks

m/z	Z	Abund	Abund %	m/z (Calc)	Diff (ppm)	Ion Species	Formula	Ion Type
325.1035		1275109	2.96					
367.1395	1	43088320	100.00					
367.2972	1	5299596	12.30					
368.1375	1	15027121	34.88					
368.3042	1	1247046	2.89					
369.1395	1	1751392	4.06					

Figure S4.B LC-MS spectra for Compound 48.

Compound 50

3-(2-(cyclohexylamino)pyridin-4-yl)-2-(4-fluorophenyl)-4,5-dihydropyrazolo[1,5-a]pyrazin-6(7H)-one
 $^1\text{H NMR}$ (400 MHz, $\text{DMSO-}d_6$) δ ppm 8.54 (s, 1 H), 7.85 - 7.90 (m, 1 H), 7.39 - 7.48 (m, 2 H), 7.15 - 7.25 (m, 2 H), 6.32 (d, $J=7.63$ Hz, 1 H), 6.16 - 6.23 (m, 2 H), 4.78 (s, 2 H), 4.48 (s, 2 H), 3.50 - 3.56 (m, 1 H), 3.47 - 3.50 (m, 1 H), 1.79 - 1.91 (m, 2 H), 1.62 - 1.72 (m, 2 H), 1.51 - 1.61 (m, 1 H), 1.21 - 1.30 (m, 2 H), 1.04 - 1.18 (m, 3 H). $[\text{M}+\text{H}]^+ = 406.16$, calculated exact mass for $\text{C}_{23}\text{H}_{25}\text{FN}_5\text{O} = 406.20$; purity 98%; $t_{\text{R}} = 2.254$ min.

$^1\text{H NMR}$ (400 MHz, $\text{DMSO-}d_6$) δ ppm 8.54 (s, 1 H), 7.85 - 7.90 (m, 1 H), 7.39 - 7.48 (m, 2 H), 7.15 - 7.25 (m, 2 H), 6.32 (d, $J=7.63$ Hz, 1 H), 6.16 - 6.23 (m, 2 H), 4.78 (s, 2 H), 4.48 (s, 2 H), 3.50 - 3.56 (m, 1 H), 3.47 - 3.50 (m, 1 H), 1.79 - 1.91 (m, 2 H), 1.62 - 1.72 (m, 2 H), 1.51 - 1.61 (m, 1 H), 1.21 - 1.30 (m, 2 H), 1.04 - 1.18 (m, 3 H)

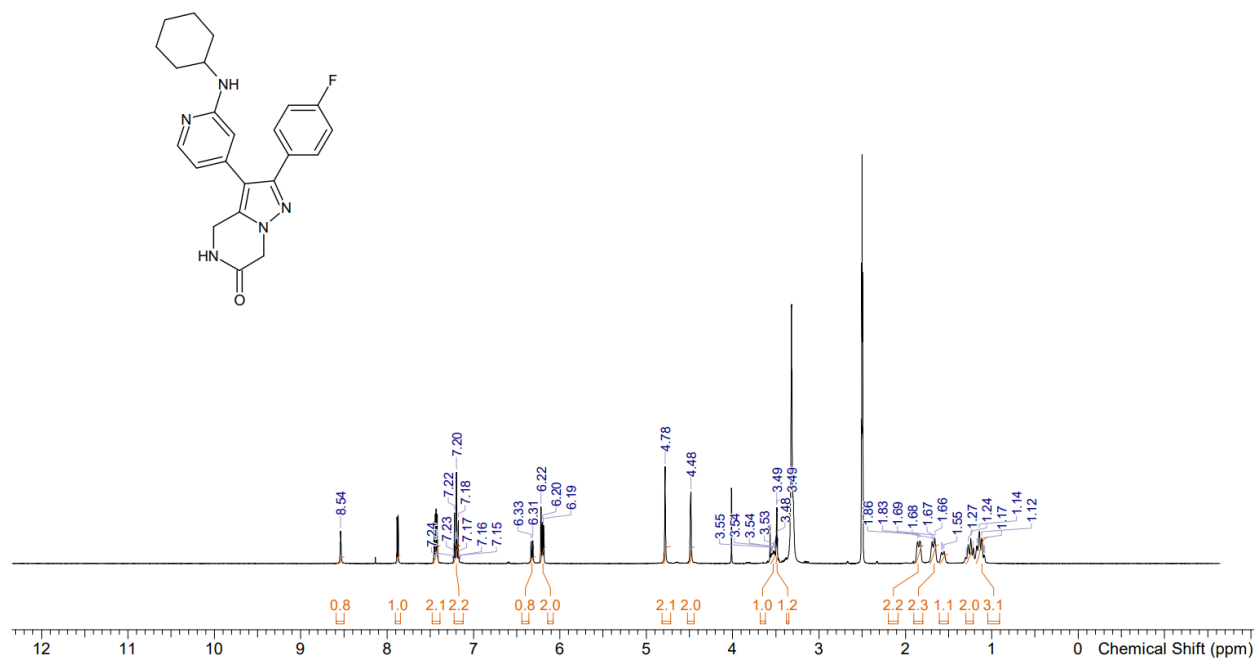
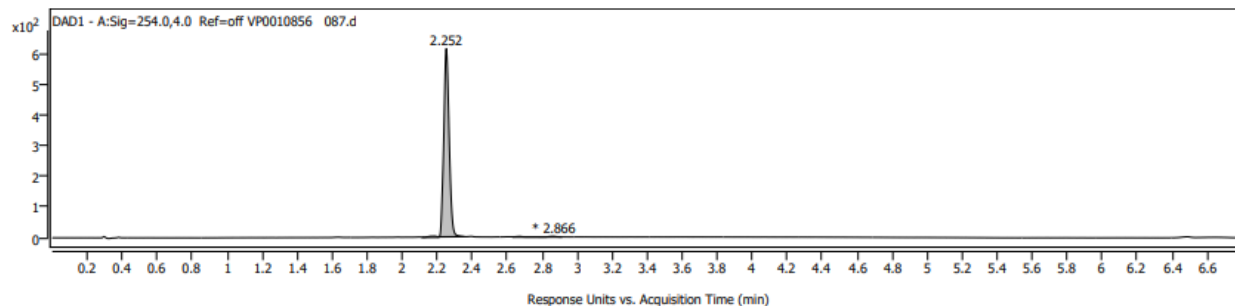
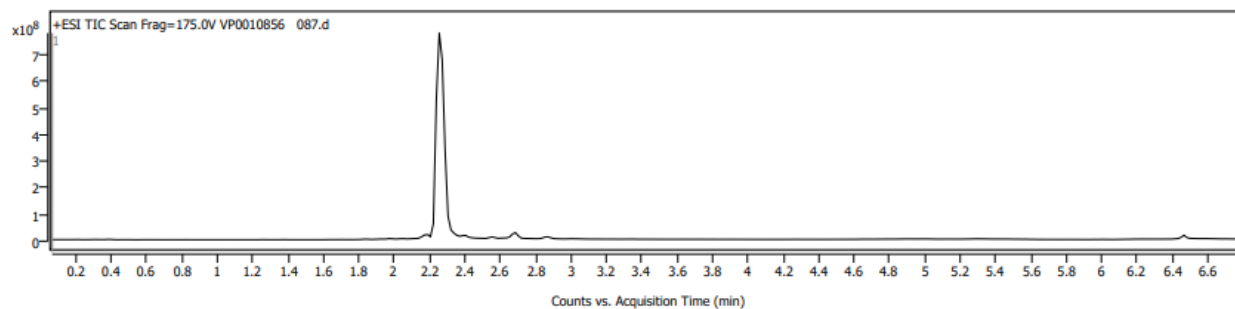


Figure S5.A $^1\text{H NMR}$ (400 MHz, $\text{DMSO-}d_6$) spectra of Compound 50.

Sample Chromatograms

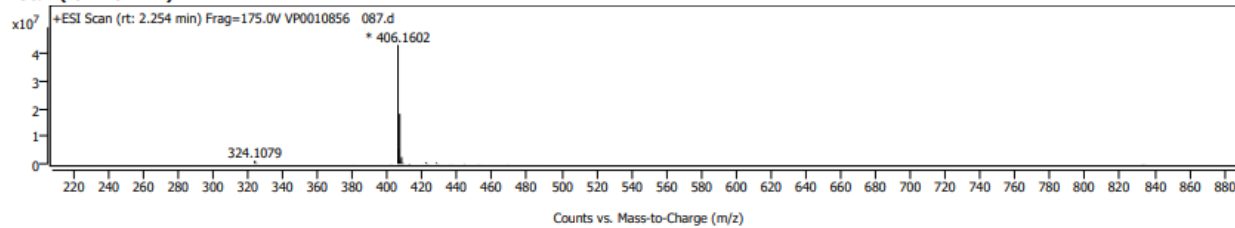


Chromatogram Peaks

Peak	Start	RT	End	Height	Area	Area Sum %
1	2.115	2.183	2.208	4	14	1.06
2	2.209	2.252	2.356	614	1312	97.82
3	2.634	2.866	2.910	2	15	1.13

Sample Spectra

+ Scan (rt: 2.254 min)



Spectrum Peaks

m/z	Z	Abund	Abund %	m/z (Calc)	Diff (ppm)	Ion Species	Formula	Ion Type
324.1079		1134115	2.62					
406.1602	1	43227780	100.00					
406.3292	1	5449052	12.61					
407.1578	1	18182132	42.06					
407.3295	1	1424281	3.29					
408.1596	1	2460707	5.69					
422.1436		503525	1.16					

Figure S5.B LC-MS spectra for Compound 50.

Compound **53**

3-(2-(cyclopropylamino)pyrimidin-4-yl)-2-(4-fluorophenyl)-4,5-dihydropyrazolo[1,5-a]pyrazin-6(7H)-one

^1H NMR (400 MHz, $\text{DMSO-}d_6$) δ ppm 8.57 - 8.65 (m, 1 H), 8.05 (br d, $J=5.05$ Hz, 1 H), 7.47 - 7.55 (m, 2 H), 7.34 (d, $J=2.86$ Hz, 1 H), 7.23 - 7.31 (m, 2 H), 6.15 (d, $J=5.25$ Hz, 1 H), 4.89 (br s, 2 H), 4.77 (s, 2 H), 2.61 - 2.69 (m, 1 H), 0.67 - 0.75 (m, 2 H), 0.45 - 0.50 (m, 2 H). $[\text{M}+\text{H}]^+ = 365.12$, calculated exact mass for $\text{C}_{19}\text{H}_{18}\text{FN}_6\text{O} = 365.15$; purity 98%; $t_R = 2.046$ min.

^1H NMR (400 MHz, $\text{DMSO-}d_6$) δ ppm 8.57 - 8.65 (m, 1 H), 8.05 (br d, $J=5.05$ Hz, 1 H), 7.47 - 7.55 (m, 2 H), 7.34 (d, $J=2.86$ Hz, 1 H), 7.23 - 7.31 (m, 2 H), 6.15 (d, $J=5.25$ Hz, 1 H), 4.89 (br s, 2 H), 4.77 (s, 2 H), 2.61 - 2.69 (m, 1 H), 0.67 - 0.75 (m, 2 H), 0.45 - 0.50 (m, 2 H)

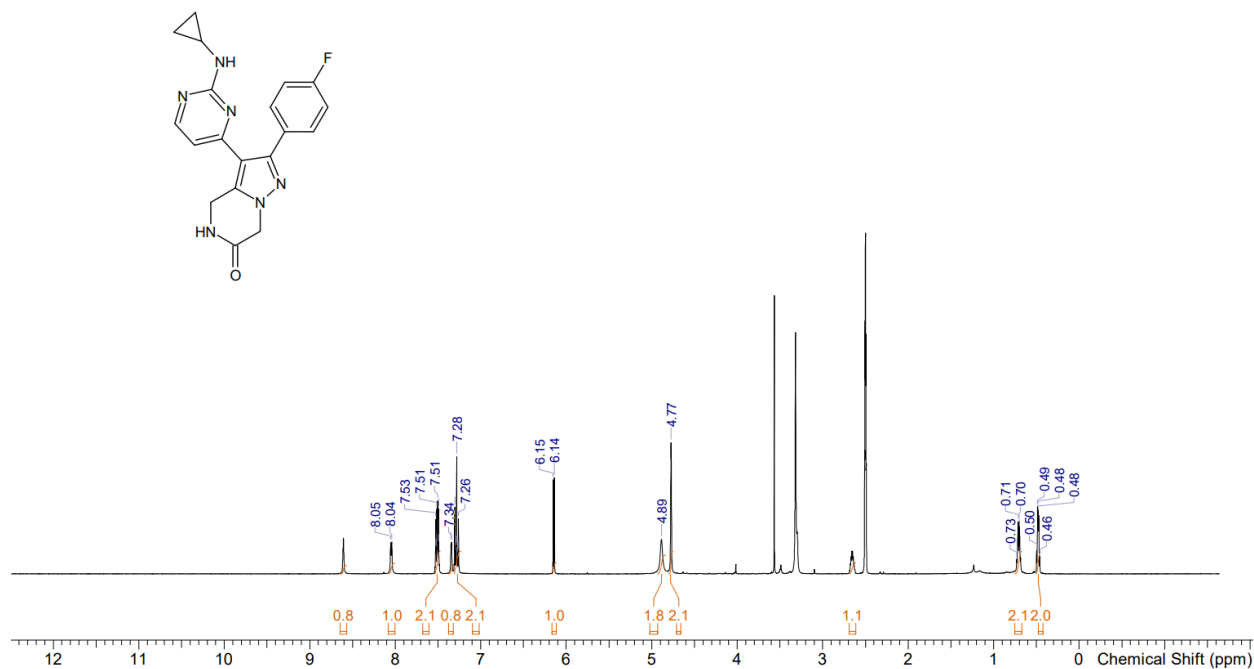
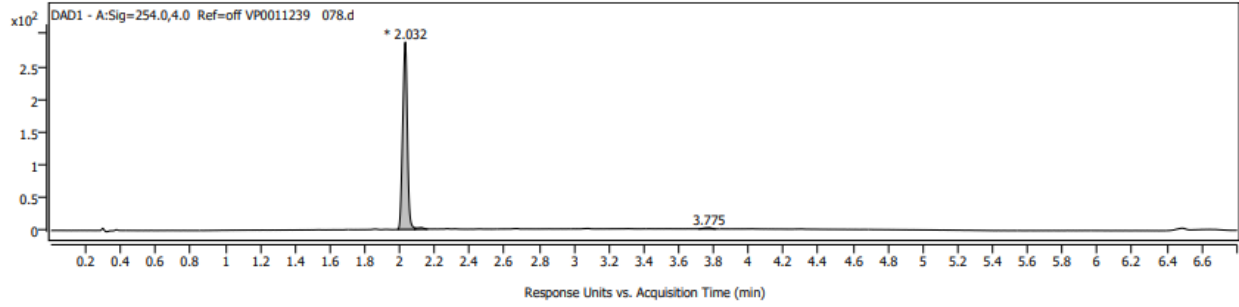
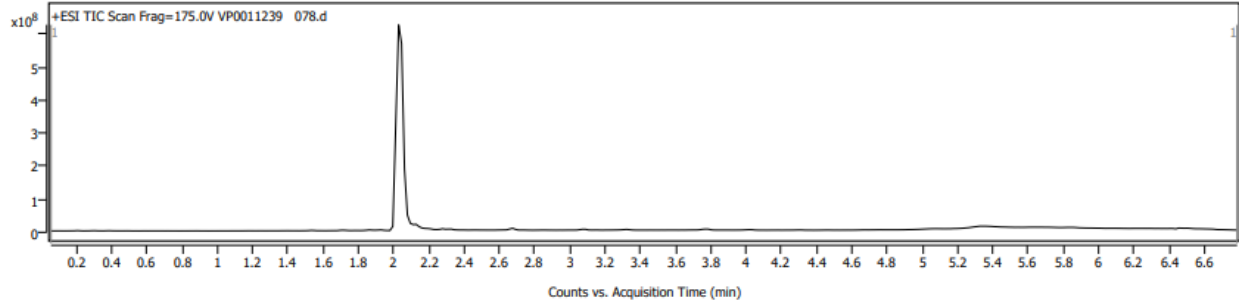


Figure S6.A ^1H NMR (400 MHz, $\text{DMSO-}d_6$) spectra of Compound **53**.

Sample Chromatograms

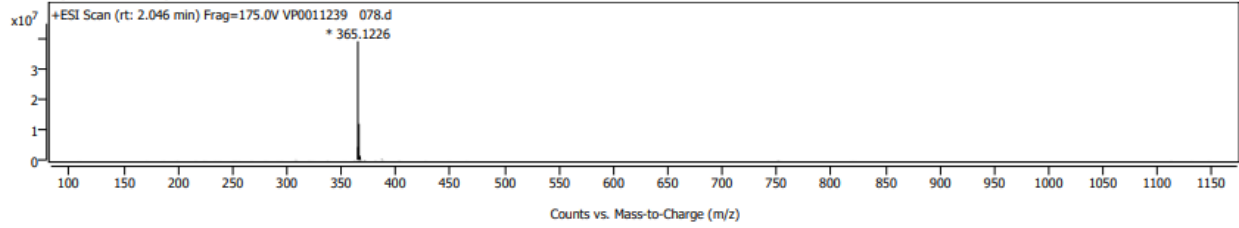


Chromatogram Peaks

Peak	Start	RT	End	Height	Area	Area Sum %
1	1.987	2.032	2.088	285	532	97.56
2	2.088	2.123	2.158	3	8	1.42
3	3.717	3.775	3.811	2	6	1.03

Sample Spectra

+ Scan (rt: 2.046 min)



Spectrum Peaks

m/z	Z	Abund	Abund %	m/z (Calc)	Diff (ppm)	Ion Species	Formula	Ion Type
365.1226	1	39280704	100.00					
365.2861	1	4254160	10.83					
366.1222	1	11941418	30.40					
366.2872	1	960453	2.45					
367.1246	1	1335036	3.40					

Figure S6.B LC-MS spectra for Compound **53**.

ADMET Characterization

Protein Binding

Plasma protein binding was determined using equilibrium dialysis in a 96-well Teflon-based format. Human plasma spiked with 10 μM of the test compound (1% DMSO) was dialyzed against phosphate-buffered saline (PBS, pH 7.4) at 37 °C for 4 hours. LC/MS/MS analysis was used to quantify the compound in both the protein and buffer compartments. Fraction unbound was determined, and control compounds (Acebutolol, Quinidine, and Warfarin) were included to assess compound stability and nonspecific adsorption.

Aqueous Solubility

Solubility was assessed by incubating the compound (200 μM , 2% DMSO) in several aqueous media, including PBS (pH 7.4), simulated gastric fluid (pH ~2), and simulated intestinal fluid (pH 7.5). After a 24-hour incubation at room temperature, samples were centrifuged, and the supernatants were analyzed by LC/UV/MS. Solubility values were calculated relative to a calibration standard. Reference control compounds (diethylstilbestrol, disulfiram, metoprolol, phenytoin, rifampicin, simvastatin, and tamoxifen) were included to verify assay performance across a range of solubility values.

Partition Coefficient (LogD)

The distribution coefficient (log D) was evaluated using a shake-flask method in a 96-well plate. The compound (100 μM) was partitioned between n-octanol and PBS (pH 7.4) for 2 hours at room temperature. Following phase separation by centrifugation, concentrations in each phase were determined by LC/UV/MS. Log D was calculated as the logarithmic ratio of compound concentrations in the octanol and aqueous phases. Reference compounds with established log D values (diethylstilbestrol, haloperidol, ketoconazole, metoprolol, phenytoin, rifampicin, simvastatin, and tamoxifen) were included as assay controls to verify method performance.

Caco-2 Permeability

Bidirectional permeability (A→B and B→A) was measured in Caco-2 monolayers (C2BBE1 clone, ATCC CRL-2102) cultured on 96-well Transwell plates, 21–25 days post-seeding. The compound (10 μM , 1% DMSO) was applied in HBSS buffer and incubated at 37 °C for either 60 min (A→B) or 40 min (B→A). For P-glycoprotein inhibition studies, 100 μM verapamil was included. LC/MS/MS was used to quantify compound transport, and fluorescein permeability was measured to verify monolayer integrity. Reference compounds (colchicine, labetalol, propranolol, and ranitidine) were included as permeability controls to verify assay performance.

Half-life in Human Plasma

Plasma stability was assessed by incubating the test compound at 1 μM (0.5% DMSO) in human plasma at 37 °C. Aliquots were taken at 0, 0.5, 1, 1.5, and 2 hours, quenched with acetonitrile, and centrifuged. The supernatants were analyzed by LC/MS/MS, and the percentage of compound remaining was used to calculate half-life, assuming first-order kinetics. Reference

compounds (propranolol and propoxycaïne) were included as stability controls to verify assay performance.

Intrinsic Clearance

Intrinsic clearance was evaluated in pooled human liver S9 fractions (1 mg/mL). The test compound (0.5 μ M) was incubated with a cofactor mixture (UDPGA, glutathione, and PAPS) at 37 °C. Reactions were initiated by adding an NADPH-generating system and stopped at defined time points (0–90 min). LC/MS/MS quantification enabled determination of compound degradation, from which half-life and intrinsic clearance (Cl_{int}) values were calculated. Reference compounds (imipramine, propranolol, terfenadine, and verapamil) were included as metabolic stability controls to verify assay performance.

CYP3A Inhibition

The evaluation of CYP3A inhibition utilized pooled human liver microsomes (0.1 mg/mL; mixed gender, 50 donors) suspended in phosphate buffer (pH 7.4). Test compounds (10 μ M) were co-incubated with CYP3A probe substrates midazolam and testosterone for 5 minutes at 37°C. Following the addition of an NADPH-generating system, reactions proceeded for 10 minutes. Samples were terminated using acetonitrile/methanol, centrifuged, and subjected to LC/MS/MS analysis to quantify 1-hydroxymidazolam and 6 β -hydroxytestosterone production. Inhibition potency was calculated relative to vehicle controls, with ketoconazole serving as the reference inhibitor.

Kinase Selectivity Assay

Kinome profiling was performed using a large-scale kinase binding assay (KINOMEScan® platform, DiscoverX Corporation). Kinase-tagged T7 phage strains were cultured in parallel using a 24-well block format in an *E. coli* host derived from the BL21 strain. The *E. coli* cultures were grown to the log phase before being infected with T7 phage from a frozen stock at a multiplicity of infection (MOI) of 0.4. The cultures were incubated at 32°C with shaking until lysis occurred (90–150 minutes). After lysis, the crude lysates were centrifuged at 6,000 \times g and filtered (0.2 μ m) to remove cellular debris. In addition to the phage-derived kinases, HEK-293 cells were used to express certain kinases, which were subsequently tagged with DNA to enable qPCR-based detection.

To prepare the affinity resins for kinase binding assays, streptavidin-coated magnetic beads were incubated for 30 minutes at room temperature with biotinylated small-molecule ligands. After ligand immobilization, the beads were blocked with excess biotin and washed with a blocking buffer (containing SeaBlock (Pierce), 1% BSA, 0.05% Tween 20, and 1 mM DTT) to remove unbound ligand and minimize non-specific phage binding.

For the kinase binding reactions, kinases, liganded affinity beads, and test compounds were combined in a 1 \times binding buffer (composed of 20% SeaBlock, 0.17 \times PBS, 0.05% Tween 20, and 6 mM DTT). Test compounds were prepared as 40 \times stock solutions in 100% DMSO and directly

diluted into the assay mixture. All reactions were conducted in polypropylene 384-well plates, with a final reaction volume of 20 μ L, and incubated for 1 hour at room temperature with shaking.

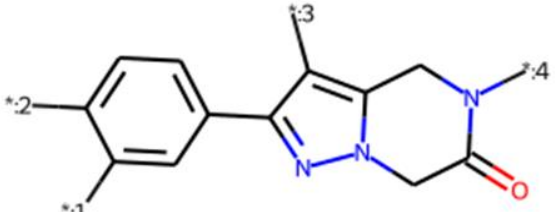
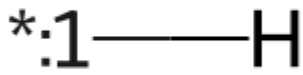
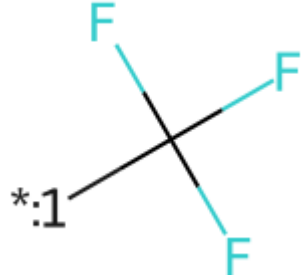

Following incubation, the affinity beads were washed with a wash buffer (1 \times PBS, 0.05% Tween 20) to remove unbound kinases. The bound kinases were then eluted by resuspending the beads in an elution buffer (1 \times PBS, 0.05% Tween 20, 0.5 μ M non-biotinylated affinity ligand) and incubating for 30 minutes at room temperature with shaking. The concentration of kinases in the eluates was subsequently measured using qPCR.



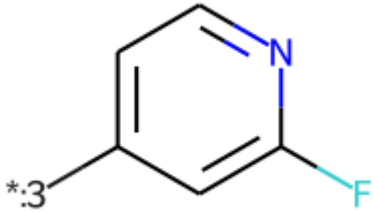
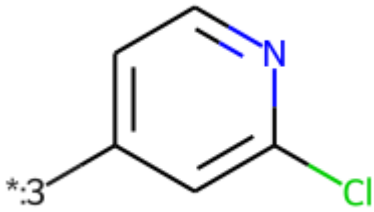
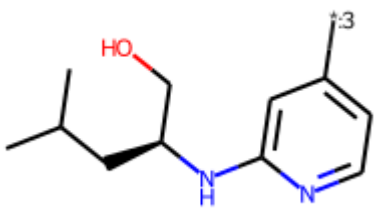
DMSO was used as the negative control (100% control signal), while an internal reference inhibitor provided within the KINOMEscan assay platform served as the positive control (0% control signal).

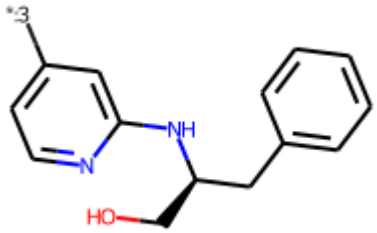
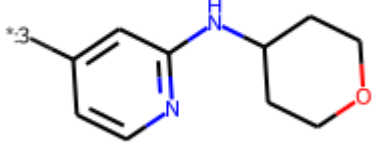
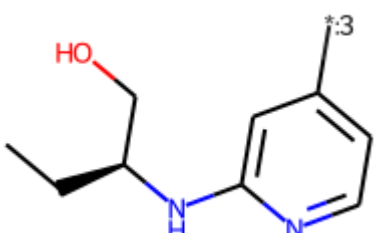
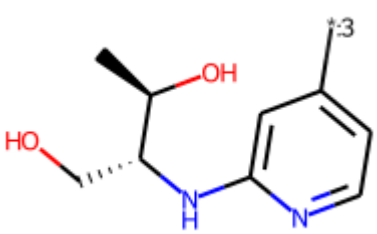
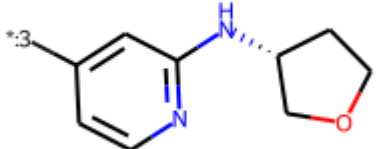
Kinome profiling results were visualized using a phylogenetic kinase tree representation (TREEspot™ software, DiscoverX Corporation). The resulting images were generated and reprinted with permission. © DISCOVERX CORPORATION 2010.

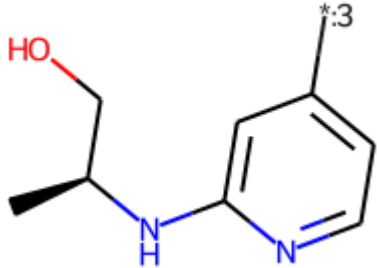
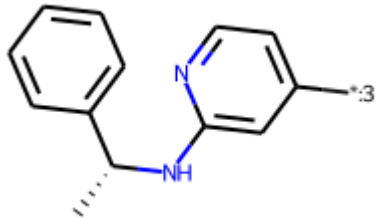
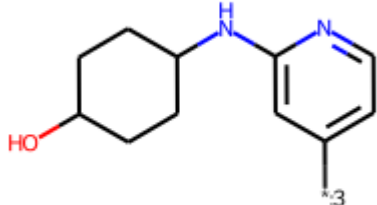
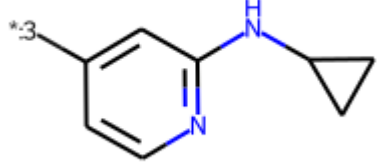
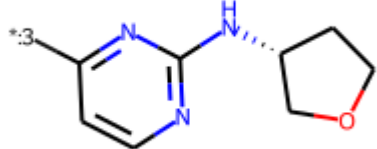
Full MolSHAP Analysis of Substituent Contributions

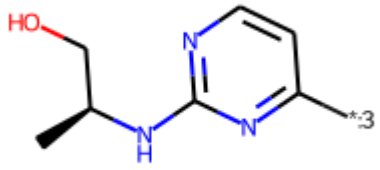
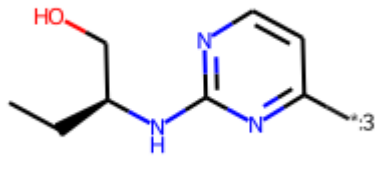
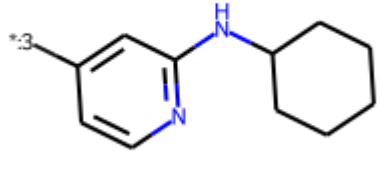
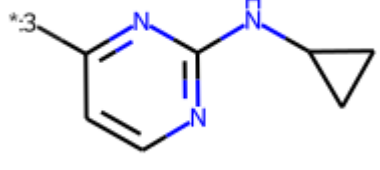
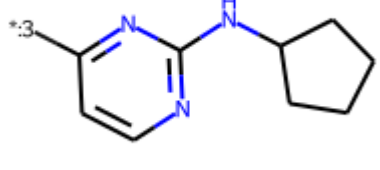
Table S1. MolSHAP-Predicted Substructure Contributions to Compound Activity (pIC₅₀).

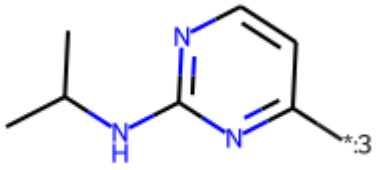
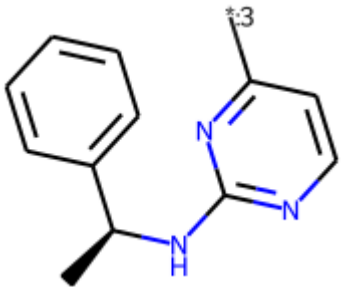
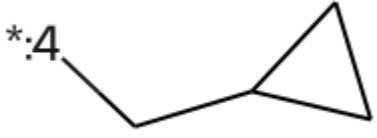
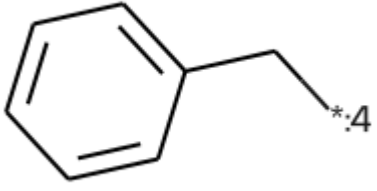

Compound Structure	Predicted pIC ₅₀ Contribution	R-Group Number
	0	Main Scaffold
	0	1
	+0.299	1
	0	2

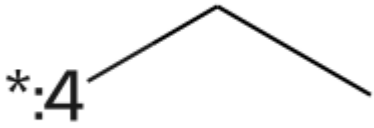

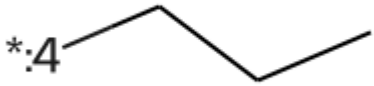
 <p>*:2—Cl</p>	+0.018	2
 <p>*:2—F</p>	+0.136	2
 <p>*:3</p>	0	3
 <p>*:3</p>	+0.032	3
 <p>*:3</p>	+0.571	3

 <p>Chemical structure of a 3-methylpyridine derivative. The pyridine ring has a methyl group (CH₃) at the 3-position. The nitrogen atom is connected to a benzyl group (-CH₂-C₆H₅) and a hydroxyl group (-OH) via a nitrogen atom.</p>	+0.867	3
 <p>Chemical structure of a 3-methylpyridine derivative. The pyridine ring has a methyl group (CH₃) at the 3-position. The nitrogen atom is connected to a piperidine ring via a nitrogen atom.</p>	+0.980	3
 <p>Chemical structure of a 3-methylpyridine derivative. The pyridine ring has a methyl group (CH₃) at the 3-position. The nitrogen atom is connected to a 1-hydroxyethyl group (-CH(OH)-CH₃) via a nitrogen atom.</p>	+1.03	3
 <p>Chemical structure of a 3-methylpyridine derivative. The pyridine ring has a methyl group (CH₃) at the 3-position. The nitrogen atom is connected to a 1,2-dihydroxyethyl group (-CH(OH)-CH₂-OH) via a nitrogen atom.</p>	+1.155	3
 <p>Chemical structure of a 3-methylpyridine derivative. The pyridine ring has a methyl group (CH₃) at the 3-position. The nitrogen atom is connected to a tetrahydrofuran ring via a nitrogen atom.</p>	+1.174	3

	+1.313	3
	+1.518	3
	+1.600	3
	+1.878	3
	+1.909	3

	+2.108	3
	+2.149	3
	+2.319	3
	+2.466	3
	+2.664	3

	+2.841	3
	+3.135	3
	-0.851	4
	-0.603	4
	-0.484	4

	-0.012	4
	0	4
	+0.121	4

Notes: Asterisk (*) denotes the R-group attachment point on the core scaffold. The numbered attachment positions (:1, *:2, *:3, *:4) are defined in the first row ("Main Scaffold") and correspond to the R-group numbering used throughout the table.

Full ADME Profiling Data of Key Compounds

Table S2. ADME Profiling Data for Selected Compounds 26, 28, 47, 48, 50, and 53.

Table S2.A Protein binding (plasma, human)

		% Protein Bound			% Recovery		
Compound	Test Concentration (M)	1st	2nd	Mean	1st	2nd	Mean
Compound 26	1.00E-05	83.43	81.87	82.65	113.66	114.71	114.18
Compound 28	1.00E-05	83.37	81.18	82.27	116.50	111.96	114.23
Compound 47	1.00E-05	94.22	96.31	95.27	112.10	106.43	109.26
Compound 48	1.00E-05	88.52	87.94	88.23	117.62	111.35	114.48
Compound 50	1.00E-05	97.68	93.12	95.40	119.95	109.73	114.84
Compound 53	1.00E-05	88.52	87.94	88.23	117.62	111.35	114.48
Acebutolol	1.00E-05	24.2	35.83	30.01	124.52	115.01	119.76
Quinidine	1.00E-05	70.53	68.02	69.28	127.77	115.78	121.78
Warfarin	1.00E-05	91.65	94.98	93.32	121.85	109.46	115.65

Table S2.B Aqueous solubility (PBS, pH 7.4)

		Solubility (µM)		
Compound	Test Concentration (M)	1st	2nd	Mean
Compound 26	2.00E-04	196.44	199.26	197.85
Compound 28	2.00E-04	195.52	197.58	196.55
Compound 47	2.00E-04	73.38	78.75	76.06
Compound 48	2.00E-04	15.30	12.37	13.83
Compound 50	2.00E-04	44.86	15.38	30.12
Compound 53	2.00E-04	17.33	24.18	20.76
Diethylstilbestrol	2.00E-04	11.91	4.16	8.03
Disulfiram	2.00E-04	55.06	52.97	54.01
Metoprolol	2.00E-04	201.53	203.49	202.51
Phenytoin	2.00E-04	83.79	86.66	85.23
Rifampicin	2.00E-04	186.34	187.44	186.89
Simvastatin	2.00E-04	20.44	20.78	20.61
Tamoxifen	2.00E-04	2.18	2.65	2.41

Table S2.C Partition coefficient (log D, n-octanol/PBS, pH 7.4). BQA indicates below the Limit of Quantitation in Aqueous phase

Compound	Test Concentration (M)	LogD	Flag
Compound 26	1.00E-04	2.07	
Compound 28	1.00E-04	2.89	
Compound 47	1.00E-04	3.22	
Compound 48	1.00E-04	2.04	
Compound 50	1.00E-04	2.59	
Compound 53	1.00E-04	2.64	
Diethylstilbestrol	1.00E-04	>4.66	BQA
Haloperidol	1.00E-04	2.67	
Ketoconazole	1.00E-04	3.57	
Metoprolol	1.00E-04	-0.34	
Phenytoin	1.00E-04	2.60	
Rifampicin	1.00E-04	1.25	
Simvastatin	1.00E-04	>4.51	BQA
Tamoxifen	1.00E-04	>4.88	BQA

Table S2.D A-B permeability (Caco-2, pH 7.4/7.4 + verapamil)

Compound	Test Concentration (M)	Permeability (10^{-6} cm/s)			% Recovery		
		1st	2nd	Mean	1st	2nd	Mean
Compound 26	1.00E-05	5.95	4.65	5.3	82	77	80
Compound 28	1.00E-05	6.81	7.01	6.9	57	55	56
Compound 47	1.00E-05	10.48	9.82	10.2	26	30	28
Compound 48	1.00E-05	12.53	10.33	11.4	43	46	45
Compound 50	1.00E-05	3.10	3.34	3.2	23	17	20
Compound 53	1.00E-05	13.03	11.00	12.0	53	49	51
Colchicine	1.00E-05	0.32	0.26	0.3	104	84	94
Labetalol	1.00E-05	15.17	15.15	15.2	69	72	70
Propranolol	1.00E-05	22	24.65	23.3	46	44	45
Ranitidine	1.00E-05	0.79	0.91	0.9	82	86	84

Table S2.E A-B permeability (Caco-2, pH 7.4/7.4)

Compound	Test Concentration (M)	Permeability (10 ⁻⁶ cm/s)			% Recovery		
		1st	2nd	Mean	1st	2nd	Mean
Compound 26	1.00E-05	9.06	11.64	10.4	62	80	71
Compound 28	1.00E-05	21.97	23.13	22.6	66	82	74
Compound 47	1.00E-05	16.59	13.53	15.1	31	28	30
Compound 48	1.00E-05	16.37	27.24	21.8	52	58	55
Compound 50	1.00E-05	10.60	11.56	11.1	23	23	23
Compound 53	1.00E-05	20.07	19.50	19.8	66	68	67
Colchicine	1.00E-05	0.29	0.25	0.3	83	85	84
Labetalol	1.00E-05	14.77	14.77	14.8	74	76	75
Propranolol	1.00E-05	58.89	58.02	58.5	61	61	61
Ranitidine	1.00E-05	1.54	1.5	1.5	91	107	99

Table S2.F B-A permeability (Caco-2, pH 7.4/7.4 + verapamil)

Compound	Test Concentration (M)	Permeability (10 ⁻⁶ cm/s)			% Recovery		
		1st	2nd	Mean	1st	2nd	Mean
Compound 26	1.00E-05	28.23	27.81	28.0	66	83	75
Compound 28	1.00E-05	15.64	14.03	14.8	59	52	55
Compound 47	1.00E-05	2.84	2.55	2.7	12	13	13
Compound 48	1.00E-05	15.72	13.29	14.5	53	43	48
Compound 50	1.00E-05	2.71	1.37	2.0	35	23	29
Compound 53	1.00E-05	23.05	18.87	21.0	57	69	63
Colchicine	1.00E-05	1.22	1.42	1.3	129	119	124
Labetalol	1.00E-05	9.16	9.16	9.2	76	76	76
Propranolol	1.00E-05	20.91	19.61	20.3	89	86	87
Ranitidine	1.00E-05	0.47	0.29	0.4	54	78	66

Table S2.G B-A permeability (Caco-2, pH 7.4/7.4)

Compound	Test Concentration (M)	Permeability (10 ⁻⁶ cm/s)			% Recovery		
		1st	2nd	Mean	1st	2nd	Mean
Compound 26	1.00E-05	19.72	19.76	19.7	25	25	25
Compound 28	1.00E-05	15.13	14.33	14.7	27	26	26
Compound 47	1.00E-05	1.55	1.59	1.6	11	10	10
Compound 48	1.00E-05	10.98	11.61	11.3	27	28	28
Compound 50	1.00E-05	3.27	2.99	3.1	35	38	36
Compound 53	1.00E-05	15.07	14.86	15.0	25	24	24
Colchicine	1.00E-05	4.34	4.33	4.3	43	53	48
Labetalol	1.00E-05	21.18	21.52	21.4	57	61	59
Propranolol	1.00E-05	19.23	17.75	18.5	68	73	70
Ranitidine	1.00E-05	3.62	3.12	3.4	68	96	82

Table S2.H Half-life in Human Plasma

Compound	Test Concentration (M)	Incubation (Min)	% Compound Remaining			Half-Life (Min)		
			1st	2nd	Mean	1st	2nd	Mean
Compound 26	1.00E-06	0	100.00	100.00	100.00	>120	>120	>120
Compound 26	1.00E-06	30	114.19	109.60	111.89			
Compound 26	1.00E-06	60	115.40	124.77	120.08			
Compound 26	1.00E-06	90	106.58	103.90	105.24			
Compound 26	1.00E-06	120	118.47	102.61	110.54			
Compound 28	1.00E-06	0	100.00	100.00	100.00	>120	>120	>120
Compound 28	1.00E-06	30	106.21	120.58	113.40			
Compound 28	1.00E-06	60	98.51	122.43	110.47			
Compound 28	1.00E-06	90	94.30	108.28	101.29			
Compound 28	1.00E-06	120	115.69	116.96	116.32			
Compound 47	1.00E-06	0	100.00	100.00	100.00	>120	>120	>120
Compound 47	1.00E-06	30	107.99	107.43	107.71			
Compound 47	1.00E-06	60	104.71	/	104.71			
Compound 47	1.00E-06	90	87.76	106.11	96.93			

Compound 47	1.00E-06	120	123.24	109.01	116.13			
Compound 48	1.00E-06	0	100.00	100.00	100.00	>120	>120	>120
Compound 48	1.00E-06	30	102.30	98.49	100.39			
Compound 48	1.00E-06	60	102.70	110.14	106.42			
Compound 48	1.00E-06	90	90.72	93.70	92.21			
Compound 48	1.00E-06	120	116.02	110.68	113.35			
Compound 50	1.00E-06	0	100.00	100.00	100.00	>120	>120	>120
Compound 50	1.00E-06	30	90.81	84.37	87.59			
Compound 50	1.00E-06	60	100.97	105.46	103.22			
Compound 50	1.00E-06	90	112.86	89.45	101.16			
Compound 50	1.00E-06	120	128.58	97.88	113.23			
Compound 53	1.00E-06	0	100.00	100.00	100.00	>120	>120	>120
Compound 53	1.00E-06	30	88.98	86.56	87.77			
Compound 53	1.00E-06	60	100.64	111.12	105.88			
Compound 53	1.00E-06	90	107.05	92.41	99.73			
Compound 53	1.00E-06	120	105.33	96.49	100.91			
Proprantheline	1.00E-06					14.9	14.9	14.9
Proprantheline	1.00E-06					15.4	15.0	15.2
Propoxycaine	1.00E-06					2.5	2.4	<2.5
Propoxycaine	1.00E-06					3.3	2.8	<3.0

Table S2.I Intrinsic Clearance (Human liver microsomes)

Compound	Test Concentration (M)	Incubation (Min)	% Compound Remaining			Half-Life (Min)			Clint (µl/min/mg)
			1st	2nd	Mean	1st	2nd	Mean	
Compound 26	1.00E-07	0	100	100	100	412.0	921.5	>60	<115.5
Compound 26	1.00E-07	15	94.83	92.90	93.87				
Compound 26	1.00E-07	30	88.31	85.58	86.95				
Compound 26	1.00E-07	45	89.56	88.86	89.21				
Compound 26	1.00E-07	60	90.71	96.64	93.67				
Compound 28	1.00E-07	0	100	100	100	224.4	212.2	>60	<115.5

Compound 28	1.00E-07	15	88.41	91.23	89.82				
Compound 28	1.00E-07	30	97.25	87.27	92.26				
Compound 28	1.00E-07	45	80.94	81.77	81.36				
Compound 28	1.00E-07	60	82.90	82.68	82.79				
Compound 47	1.00E-07	0	100	100	100	17.2	16.5	16.8	411.9
Compound 47	1.00E-07	15	57.90	56.94	57.42				
Compound 47	1.00E-07	30	28.23	24.99	26.61				
Compound 47	1.00E-07	45	16.32	13.38	14.85				
Compound 47	1.00E-07	60	9.10	8.84	8.97				
Compound 48	1.00E-07	0	100	100	100	321.3	242.2	>60	<115.5
Compound 48	1.00E-07	15	91.33	94.02	92.67				
Compound 48	1.00E-07	30	88.10	87.79	87.95				
Compound 48	1.00E-07	45	89.73	89.59	89.66				
Compound 48	1.00E-07	60	85.82	82.65	84.23				
Compound 50	1.00E-07	0	100	100	100	5.2	5.1	5.1	1347.5
Compound 50	1.00E-07	15	17.00	14.95	15.97				
Compound 50	1.00E-07	30	1.86	1.65	1.76				
Compound 50	1.00E-07	45	0.57	0.57	0.57				
Compound 50	1.00E-07	60	0.44	0.34	0.39				
Compound 53	1.00E-07	0	100	100	100	195.5	155.3	>60	<115.5
Compound 53	1.00E-07	15	84.77	87.32	86.04				
Compound 53	1.00E-07	30	79.08	80.30	79.69				
Compound 53	1.00E-07	45	78.84	81.99	80.41				
Compound 53	1.00E-07	60	79.48	73.85	76.67				
Imipramine	1.00E-07					372.1	148.4	>60	<115.5
Propranolol	1.00E-07					182.5	183.3	>60	<115.5
Terfenadine	1.00E-07					11.4	11.2	11.3	614.3
Verapamil	1.00E-07					42.8	44.6	43.7	158.7

Table S2.J CYP3A inhibition with 5 µM Midazolam

Compound	Test Concentration (M)	% Inhibition of Control Values		
		1st	2nd	Mean
Compound 26	1.00E-05	5.9	2.6	4.3
Compound 28	1.00E-05	11.1	16.2	13.7
Compound 47	1.00E-05	56.6	57.9	57.3
Compound 48	1.00E-05	2.5	7.1	4.8
Compound 50	1.00E-05	-8.6	3.8	-2.4
Compound 53	1.00E-05	1.9	9.1	5.5
Ketoconazole	3.00E-09			-0.9
Ketoconazole	3.00E-08			10.4
Ketoconazole	1.00E-07			46.4
Ketoconazole	3.00E-07			77.2
Ketoconazole	1.00E-06			92.2
Ketoconazole	1.00E-05			99

Table S2.K CYP3A inhibition with 50 µM Testosterone

Compound	Test Concentration (M)	% Inhibition of Control Values		
		1st	2nd	Mean
Compound 26	1.00E-05	20.6	15.4	18.0
Compound 28	1.00E-05	29.2	25.4	27.3
Compound 47	1.00E-05	54.3	45.9	50.1
Compound 48	1.00E-05	12.2	25.5	18.9
Compound 50	1.00E-05	33.1	24.2	28.6
Compound 53	1.00E-05	17.9	15.8	16.9
Ketoconazole	3.00E-09			1.0
Ketoconazole	3.00E-08			11.2
Ketoconazole	1.00E-07			46.6
Ketoconazole	3.00E-07			86.3
Ketoconazole	1.00E-06			95.6
Ketoconazole	1.00E-05			97.9

Full KINOMEscan Binding Profile of Compound 26

Table S3. Full Kinase Binding Profile of Compound 26 from KINOMEscan™ Assay at 100 nM and 1,000 nM.

KINOMEscan Gene Symbol	Percent Control (100 nM)	Percent Control (1,000 nM)
AAK1	100	97
ABL1(E255K)-phosphorylated	89	89
ABL1(F317I)-nonphosphorylated	100	100
ABL1(F317I)-phosphorylated	96	94
ABL1(F317L)-nonphosphorylated	100	100
ABL1(F317L)-phosphorylated	88	76
ABL1(H396P)-nonphosphorylated	100	100
ABL1(H396P)-phosphorylated	95	82
ABL1(M351T)-phosphorylated	90	87
ABL1(Q252H)-nonphosphorylated	100	100
ABL1(Q252H)-phosphorylated	83	68
ABL1(T315I)-nonphosphorylated	100	100
ABL1(T315I)-phosphorylated	92	91
ABL1(Y253F)-phosphorylated	95	91
ABL1-nonphosphorylated	90	87
ABL1-phosphorylated	92	87
ABL2	100	100
ACVR1	100	95
ACVR1B	100	100
ACVR2A	99	100
ACVR2B	92	76
ACVRL1	100	97
ADCK3	93	78
ADCK4	80	34
AKT1	100	100
AKT2	100	100
AKT3	100	100
ALK	72	96

ALK(C1156Y)	100	100
ALK(L1196M)	96	100
AMPK-alpha1	98	100
AMPK-alpha2	100	100
ANKK1	88	83
ARK5	100	100
ASK1	100	100
ASK2	97	94
AURKA	84	90
AURKB	80	81
AURKC	95	100
AXL	98	100
BIKE	99	100
BLK	100	100
BMPR1A	100	100
BMPR1B	80	88
BMPR2	89	98
BMX	90	88
BRAF	83	66
BRAF(V600E)	81	60
BRK	100	99
BRSK1	100	100
BRSK2	84	81
BTK	83	84
BUB1	83	49
CAMK1	93	84
CAMK1B	79	91
CAMK1D	100	98
CAMK1G	99	100
CAMK2A	100	100
CAMK2B	100	100

CAMK2D	100	100
CAMK2G	100	93
CAMK4	96	96
CAMKK1	100	83
CAMKK2	100	90
CASK	94	100
CDC2L1	100	83
CDC2L2	90	67
CDC2L5	77	91
CDK11	97	100
CDK2	97	100
CDK3	98	95
CDK4	96	99
CDK4-cyclinD1	96	97
CDK4-cyclinD3	100	100
CDK5	100	100
CDK7	100	100
CDK8	97	100
CDK9	100	100
CDKL1	100	98
CDKL2	100	87
CDKL3	92	100
CDKL5	86	83
CHEK1	100	100
CHEK2	100	94
CIT	71	7.8
CLK1	86	90
CLK2	100	100
CLK3	93	98
CLK4	100	100
CSF1R	99	94

CSF1R-autoinhibited	92	100
CSK	100	100
CSNK1A1	36	2.1
CSNK1A1L	90	49
CSNK1D	3.1	2.3
CSNK1E	1.8	0.1
CSNK1G1	88	55
CSNK1G2	98	34
CSNK1G3	80	26
CSNK2A1	79	89
CSNK2A2	88	87
CTK	87	95
DAPK1	92	96
DAPK2	100	93
DAPK3	100	100
DCAMKL1	74	78
DCAMKL2	92	92
DCAMKL3	97	100
DDR1	50	2.8
DDR2	49	14
DLK	92	97
DMPK	100	94
DMPK2	67	20
DRAK1	97	88
DRAK2	99	92
DYRK1A	92	95
DYRK1B	70	100
DYRK2	76	83
EGFR	90	76
EGFR(E746-A750del)	76	74
EGFR(G719C)	100	91

EGFR(G719S)	100	95
EGFR(L747-E749del_A750P)	91	81
EGFR(L747-S752del_P753S)	67	65
EGFR(L747-T751del_Sins)	100	89
EGFR(L858R)	88	60
EGFR(L858R_T790M)	72	47
EGFR(L861Q)	100	92
EGFR(S752-I759del)	98	90
EGFR(T790M)	96	67
EIF2AK1	100	99
EPHA1	93	97
EPHA2	100	91
EPHA3	92	73
EPHA4	100	95
EPHA5	100	100
EPHA6	100	86
EPHA7	93	100
EPHA8	95	100
EPHB1	100	100
EPHB2	88	100
EPHB3	100	96
EPHB4	100	97
EPHB6	100	93
ERBB2	92	87
ERBB3	78	75
ERBB4	82	73
ERK1	100	100
ERK2	100	100
ERK3	76	84
ERK4	57	56
ERK5	97	94

ERK8	94	97
ERN1	87	86
FAK	94	99
FER	92	95
FES	100	100
FGFR1	94	93
FGFR2	88	91
FGFR3	99	96
FGFR3(G697C)	96	95
FGFR4	100	96
FGR	100	100
FLT1	93	99
FLT3	86	95
FLT3(D835H)	97	97
FLT3(D835V)	76	94
FLT3(D835Y)	100	100
FLT3(ITD)	92	96
FLT3(ITD_D835V)	66	74
FLT3(ITD_F691L)	47	48
FLT3(K663Q)	96	100
FLT3(N841I)	100	90
FLT3(R834Q)	100	100
FLT3-autoinhibited	94	90
FLT4	95	98
FRK	96	85
FYN	98	92
GAK	40	15
GCN2(Kin.Dom.2_S808G)	97	100
GRK1	89	80
GRK2	45	43
GRK3	100	100

GRK4	89	99
GRK7	98	89
GSK3A	95	83
GSK3B	80	83
HASPIN	96	100
HCK	100	91
HIPK1	94	89
HIPK2	88	87
HIPK3	85	87
HIPK4	100	100
HPK1	95	100
HUNK	100	100
ICK	81	73
IGF1R	100	100
IKK-alpha	83	90
IKK-beta	92	99
IKK-epsilon	92	91
INSR	96	87
INSRR	100	100
IRAK1	100	98
IRAK3	82	98
IRAK4	70	94
ITK	97	100
JAK1(JH1domain-catalytic)	100	98
JAK1(JH2domain-pseudokinase)	64	52
JAK2(JH1domain-catalytic)	93	85
JAK3(JH1domain-catalytic)	81	93
JNK1	12	0.35
JNK2	0.4	0.1
JNK3	0.7	0.05
KIT	95	100

KIT(A829P)	92	100
KIT(D816H)	55	52
KIT(D816V)	92	97
KIT(L576P)	92	95
KIT(V559D)	92	96
KIT(V559D_T670I)	96	94
KIT(V559D_V654A)	97	86
KIT-autoinhibited	92	91
LATS1	100	100
LATS2	93	88
LCK	94	96
LIMK1	100	98
LIMK2	71	80
LKB1	83	100
LOK	96	96
LRRK2	100	84
LRRK2(G2019S)	88	99
LTK	100	97
LYN	97	98
LZK	78	87
MAK	94	100
MAP3K1	89	100
MAP3K15	66	95
MAP3K2	88	86
MAP3K3	98	77
MAP3K4	91	96
MAP4K2	98	100
MAP4K3	98	100
MAP4K4	96	54
MAP4K5	100	99
MAPKAPK2	93	93

MAPKAPK5	90	100
MARK1	89	100
MARK2	98	83
MARK3	100	99
MARK4	86	93
MAST1	90	100
MEK1	65	82
MEK2	70	80
MEK3	80	88
MEK4	100	88
MEK5	71	63
MEK6	100	98
MELK	100	100
MERTK	97	100
MET	100	100
MET(M1250T)	100	100
MET(Y1235D)	100	97
MINK	70	32
MKK7	89	75
MKNK1	97	83
MKNK2	100	90
MLCK	91	79
MLK1	100	100
MLK2	98	90
MLK3	100	99
MRCKA	100	77
MRCKB	96	86
MST1	100	94
MST1R	100	100
MST2	83	89
MST3	100	72

MST4	100	100
MTOR	73	87
MUSK	100	100
MYLK	95	96
MYLK2	100	100
MYLK4	100	94
MYO3A	100	94
MYO3B	100	100
NDR1	100	83
NDR2	100	99
NEK1	100	100
NEK10	55	60
NEK11	87	95
NEK2	100	100
NEK3	77	75
NEK4	91	100
NEK5	84	86
NEK6	100	100
NEK7	100	100
NEK9	100	100
NIK	85	92
NIM1	58	66
NLK	29	9.3
OSR1	95	90
p38-alpha	0.1	0
p38-beta	34	1.2
p38-delta	90	90
p38-gamma	92	84
PAK1	95	94
PAK2	98	96
PAK3	73	78

PAK4	94	88
PAK6	98	98
PAK7	88	90
PCTK1	89	97
PCTK2	94	90
PCTK3	85	88
PDGFRA	100	100
PDGFRB	92	93
PDPK1	100	100
PFCDPK1(P.falciparum)	66	49
PFPK5(P.falciparum)	83	98
PFTAIRE2	100	100
PFTK1	94	95
PHKG1	93	95
PHKG2	98	100
PIK3C2B	97	82
PIK3C2G	81	78
PIK3CA	90	86
PIK3CA(C420R)	94	93
PIK3CA(E542K)	86	83
PIK3CA(E545A)	92	93
PIK3CA(E545K)	71	69
PIK3CA(H1047L)	77	73
PIK3CA(H1047Y)	100	100
PIK3CA(I800L)	91	78
PIK3CA(M1043I)	100	100
PIK3CA(Q546K)	72	70
PIK3CB	86	83
PIK3CD	84	91
PIK3CG	99	94
PIK4CB	77	72

PIKFYVE	84	95
PIM1	89	95
PIM2	99	100
PIM3	99	100
PIP5K1A	100	100
PIP5K1C	90	91
PIP5K2B	100	100
PIP5K2C	78	87
PKAC-alpha	100	100
PKAC-beta	96	94
PKMYT1	92	85
PKN1	100	100
PKN2	100	86
PKNB(M.tuberculosis)	86	81
PLK1	91	79
PLK2	78	82
PLK3	74	76
PLK4	94	92
PRKCD	95	100
PRKCE	67	80
PRKCH	100	96
PRKCI	100	97
PRKCQ	100	100
PRKD1	95	63
PRKD2	100	100
PRKD3	99	91
PRKG1	94	100
PRKG2	96	92
PRKR	91	94
PRKX	96	96
PRP4	100	100

PYK2	99	86
QSK	88	91
RAF1	100	97
RET	89	95
RET(M918T)	100	97
RET(V804L)	100	100
RET(V804M)	100	100
RIOK1	100	100
RIOK2	99	95
RIOK3	100	100
RIPK1	73	79
RIPK2	51	18
RIPK4	60	56
RIPK5	75	64
ROCK1	98	100
ROCK2	94	100
ROS1	98	100
RPS6KA4(Kin.Dom.1-N-terminal)	100	100
RPS6KA4(Kin.Dom.2-C-terminal)	65	72
RPS6KA5(Kin.Dom.1-N-terminal)	100	99
RPS6KA5(Kin.Dom.2-C-terminal)	100	100
RSK1(Kin.Dom.1-N-terminal)	98	90
RSK1(Kin.Dom.2-C-terminal)	85	62
RSK2(Kin.Dom.1-N-terminal)	90	76
RSK2(Kin.Dom.2-C-terminal)	86	100
RSK3(Kin.Dom.1-N-terminal)	92	100
RSK3(Kin.Dom.2-C-terminal)	100	67
RSK4(Kin.Dom.1-N-terminal)	98	99
RSK4(Kin.Dom.2-C-terminal)	100	22
S6K1	83	87
SBK1	94	92

SGK	76	77
SGK2	74	95
SGK3	99	97
SIK	100	100
SIK2	97	82
SLK	98	95
SNARK	96	84
SNRK	100	100
SRC	100	100
SRMS	89	97
SRPK1	94	77
SRPK2	100	90
SRPK3	86	87
STK16	98	92
STK33	100	100
STK35	100	100
STK36	100	58
STK39	86	91
SYK	97	88
SgK110	94	90
TAK1	95	81
TAOK1	83	37
TAOK2	93	89
TAOK3	87	72
TBK1	100	96
TEC	100	100
TESK1	81	88
TGFBR1	100	99
TGFBR2	100	88
TIE1	95	100
TIE2	100	100

TLK1	98	100
TLK2	79	77
TNIK	87	23
TNK1	100	91
TNK2	94	95
TNNI3K	98	81
TRKA	75	75
TRKB	76	58
TRKC	72	68
TRPM6	83	100
TSSK1B	100	100
TSSK3	100	100
TTK	76	62
TXK	93	91
TYK2(JH1domain-catalytic)	79	100
TYK2(JH2domain-pseudokinase)	76	78
TYRO3	94	99
ULK1	98	91
ULK2	73	100
ULK3	78	76
VEGFR2	82	72
VPS34	77	88
VRK2	82	52
WEE1	92	100
WEE2	100	100
WNK1	79	93
WNK2	71	78
WNK3	79	86
WNK4	78	96
YANK1	100	53
YANK2	100	61

YANK3	90	97
YES	92	99
YSK1	94	89
YSK4	99	96
ZAK	96	78
ZAP70	100	100